Characterizing lipid biomarkers in methanotrophic communities of gas hydrate-bearing sediments in the Sea of Okhotsk

Jin-Yong Yang [a], Kyung-Ho Chung [b], Young-Keun Jin [b], Kyung-Hoon Shin [a,*]

[a] Department of Environmental Marine Sciences, Hanyang University, Ansan 425-791, Korea
[b] Korea Polar Research Institute, KOPRI, Incheon 406-840, Korea

ARTICLE INFO

ABSTRACT

We studied specific lipid biomarkers of archaea and bacteria, that are associated with the anaerobic oxidation of methane (AOM) in a cold seep environment as well as the origin of sedimentary organic matter on the continental slope off NE Sakhalin in the Sea of Okhotsk. The organic geochemical parameters demonstrated that most of the sedimentary organic matter containing hydrate layers could be derived from marine phytoplankton and bacteria, except for a station (LV39-29H) which was remarkably affected by terrestrial vascular plant. Specific methanotrophic archaea biomarkers was vertically detected in hydrate-bearing cores (LV39-40H), coinciding with the negative excursion of the $\delta^{13}C_{org}$ at core depths of 90–100 cm below the seafloor. These results suggest that methane provided from gas hydrates are already available substrates for microbes thriving in this sediment depth. In addition, the stable isotope mass balance method revealed that approximately 2.77–3.41% of the total organic carbon (or 0.036–0.044% dry weight sediment) was generated by the activity of the AOM consortium in the corresponding depth of core LV39-40H. On the other hand, the heavier $\delta^{13}C$ values of archaeol in the gas hydrate stability zone may allow ongoing methanogenesis in deeper sediment depth.

© 2011 Elsevier Ltd. All rights reserved.

1. Introduction

Large amounts of methane, which is approximately 20 times more powerful as a greenhouse gas than CO_2, are primarily stored in marine sediments as clathrate (Wuebbles and Hayhoe, 2002; Buffett and Archer, 2004). Despite high production rates and massive reservoirs of methane in marine sediments, the global contribution of methane from the oceans to atmospheric pools is estimated to be less than 3% due to the anaerobic oxidation of methane (AOM) with sulphate as the terminal electron acceptor (Barnes and Goldberg, 1976; Reeburgh, 1996; Hinrichs and Boetius, 2002).

Even though pure cultures of AOM communities are not yet available, many researchers have provided evidence that AOM is mediated by a consortium consisting of methanotrophic *Archaea* and sulphate reducing *Bacteria* (SRB) in marine environments using various techniques. Examples of these techniques include small-subunit ribosomal RNA (16S rRNA) gene sequencing (Hinrichs et al., 1999), fluorescence *in situ* hybridization with a secondary ion mass spectrometry technique (FISH-SIMS) (Orphan et al., 2001),

an *in vitro* $^{13}CH_4$ labelling experiment (Blumenberg et al., 2005) and extremely ^{13}C-depleted carbon isotopic compositions of lipid biomarkers (Elvert et al., 1999; Hinrichs et al., 1999; Peckmann et al., 1999; Thiel et al., 1999). The strong ^{13}C-depletions of the biomarkers is a consequence of the biological isotope fractionation of the carbon substrate (methane), which is known to show extreme carbon isotope depletions (Valentine and Reeburgh, 2000; Hinrichs and Boetius, 2002; Niemann et al., 2006a,b).

The most reliable lipid biomarkers in methane-seepage sites indicative for AOM are PMI (2,6,10,15,19-pentamethylicosane), cro-cetane (2,6,11,15-tetramethylhexadecane), *sn*-2-hydroxyarchaeol (2-*O*-3-hydroxyphytanyl-3-*O*-phytanyl-*sn*-glycerol), and archaeol (2,3-di-*O*-phytanyl-*sn*-glycerol) for *Archaea*, as well as *iso*- and *anteiso*- $C_{15:0}$ and $C_{16:1\omega5}$ fatty acids and non-isoprenoidal diether lipids for SRB (Elvert et al., 1999; Hinrichs et al., 1999; Peckmann et al., 1999; Thiel et al., 1999; Pancost et al., 2001; Blumenberg et al., 2004).

Three different clades of anaerobic methanotrophs (ANME -1, -2, -3) are phylogenetically characterized by 16S rRNA gene sequences (Hinrichs et al., 1999; Orphan et al., 2002; Niemann et al., 2006a). ANME-1 and -2 archaea, which are distantly related to metha-nogens of the orders *Methanosarcinales* and *Methanomicrobiales*, are usually associated with the SRB of the *Desulfosarcina/Desulfo-coccus* branch (DSS) (Hinrichs et al., 1999; Boetius et al., 2000;

* Corresponding author. Tel.: +82 31 4005536; fax: +82 31 4166173.
E-mail address: shinkh@hanyang.ac.kr (K.-H. Shin).

Knittel et al., 2005). ANME-3 archaea, which are most closely related to the cultured *Methanococcoides* genera, serve as syntrophic partners of *Desulfobulbus* species (DBB) (Niemann et al., 2006a). Several recent studies have shown that membrane lipids from different clusters of ANMEs and SRBs are expressed by their abundance and composition of lipid biomarkers (Elvert et al., 2003, 2005; Blumenberg et al., 2004; Niemann et al., 2005). The literature database of diagnostic lipids has provided statistically relevant information, detailed information regarding the AOM consortium (Niemann and Elvert, 2008).

The Sea of Okhotsk is one of the largest marginal seas in the world and it is characterized by a region where the seasonal sea ice reaches the lowest latitudes (Kimura and Wakatsuchi, 2000). The Sea of Okhotsk is also one of the areas of the World Ocean that is highly biologically productive. In addition, it exhibits a large flux of organic carbon to the seafloor (Koblents-Mishke, 1967; Bogorov, 1974) and is characterized by high sedimentation rates (150–200 mm/ka) (Zonenshayn et al., 1987). In the present study, mud volcano and methane hydrate occurrences were associated with the active gas vents on the northeast Sakhalin Slope which were caused by high amounts of organic matter and the joint compression of the seafloor by the surrounding plates (Zonenshayn et al., 1987; Ginsburg et al., 1993; Soloviev et al., 1994; Greinert et al., 2002; Lüdmann and Wong, 2003; Shakirov et al., 2004; Shoji et al., 2005). For example, the bottom simulating reflector (BSR) from the geophysical investigation and the hydroacoustic anomalies in the water column were interpreted by examining the distribution of the methane hydrates and the signatures of the methane flumes that emanated from the seafloor, respectively (Zonenshayn et al., 1987; Ginsburg et al., 1993; Lüdmann and Wong, 2003; Jin et al., 2004; Luan et al., 2008). The methane concentrations in the water column and sediments have been measured in order to detect the locations of the gas seepage sites (Obzhirov, 1992, 1993; Obzhirov et al., 2002, 2004). Indirect indications of the presence of hydrate, such as visual observations, porewater chemistry data, and oxygen and hydrogen stable isotopic signatures ($\delta^{18}O$, δD) of the hydrate water, were also reported in the Sea of Okhotsk (Ginsburg et al., 1993; Matveeva et al., 2003). Most of the methane encaged in the hydrate and also migrating from the deep, buried reservoirs along the faulting zones in the Okhotsk Sea, was determined to be generated by microbial carbonate reduction rather than from thermogenic origin, by characterizing the composition of the hydrocarbon gases [$C_1/(C_2 + C_3)$] and the carbon and hydrogen stable isotope ratios ($\delta^{13}C$, δD) (Ginsburg et al., 1993; Matveeva et al., 2003; Mazurenko et al., 2005).

The presence of biogenic methane and AOM in the Sea of Okhotsk indicates that microbiological activities are important for the formation and dissociation of methane hydrate (Cragg et al., 1996; Wellsbury et al., 1997; Hinrichs et al., 1999; Dickens, 2003). Some previous investigation for understanding the process of AOM in this region have focused on the phylogenetic distribution of microbial communities (Inagaki et al., 2003), the symbiotic and benthic ecological aspects (Sahling et al., 2003; Pestrikova and Obzhirov, 2007), and the modelling approach for determining the organic matter flux (Wallmann et al., 2006). Much more studies also found evidence of AOM including lipid biomarkers (Peckmann et al., 1999; Thiel et al., 1999; Aloisi et al., 2004) as well as authigenic carbonate and barite precipitates with low $\delta^{13}C$ values (ca. −40‰) that were a result of the anaerobic oxidation of biogenic methane (Derkachev et al., 2000; Greinert et al., 2002; Aloisi et al., 2004; Lembke et al., 2007). The oldest record of AOM was as well found in seep-carbonates (Birgel et al., 2008). However, there have not been any studies conducted on the microbial lipid biomarkers in relation to the methane hydrate-bearing sediments in the well-known, cold seep environment (on the continental slope offshore of NE Sakhalin in the Sea of Okhotsk).

The objective of this study is to identify the origin of sedimentary organic matter and to characterize the indigenous microbial community distribution under various sediment environments in the Sea of Okhotsk (i.e. large methane flux, presence and non-presence of gas hydrate, etc.).

2. Materials and methods

2.1. Study area and sample collection

Multidisciplinary field investigations were conducted in May 2006 at the Derugin Basin in the central portion of the Sea of Okhotsk using the R/V *Akademik M.A. Lavrentyev* (LV) from the Russian Academy of Sciences (RAS). These investigations were conducted within the framework of the CHAOS project (hydro-Carbon Hydrate Accumulations in the Okhotsk Sea), which was supported by China, Japan, Korea, and Russia. Nine sediment cores were obtained from various sites (KOPRI, CHAOS, POI, GIZELLA and new gas-venting sites) using a 5.5-m gravity corer with a 126-mm diameter, lengthwise-cut split plastic liner in order to collect gas hydrate-bearing sediment (Fig. 1, Table 1).

Gas hydrates were observed at the LV39-25H and LV39-40H cores (Table 1), and the gas hydrate content in the hydrate-bearing intervals of 60–245 cm and 165–265 cm below the seafloor (cmbsf) were visually estimated to be as high as 5–10% and 15–20% by sediment volume, respectively (Luan et al., 2008). The LV39-40H core was characterized by the presence of carbonate concretions that were up to 3 cm in diameter within the core interval of 90–95 cmbsf. In addition, gas-saturated characteristics including cheese-like structures created through degassing and a strong H_2S odour were also present above the lenticular-bedded sediments from a thickness of a few millimeters to 3 cm in the hydrate-bearing zone (Fig. 2). Sub-samples were sliced into depth intervals of 10 cm and were collected in 100-ml glass bottles for organic geochemical analysis. The sub-samples were immediately frozen at −20 °C and were kept frozen until the analysis was conducted. The LV39-30H and LV39-40H cores were analyzed vertically in order to compare the organic, geochemical distinction with the existence of the gas hydrate layers.

2.2. Extraction, chromatographic separation and derivatization

Lipids were extracted from approximately 4 g freeze-dried and grinded sub-samples via sonication (Branson 5510) for 15 min at 20 °C three times in a row in a solvent mixture (15 ml) of dichloromethane/methanol (99/1, v/v). Subsequently, the aliquots of the resulting extract were concentrated using a rotary evaporator (EYELA n-1000) and then evaporated to dryness under a nitrogen gas stream.

Neutral- and polar-lipids present in the aliquots were cleaved by saponification with methanolic KOH solution. After the extraction of the neutral lipid fraction from this mixture, the carboxylic acids were obtained by acidification (HCl, pH 1–2) of the residual reaction mixture and extraction with *n*-hexane instead of water. The hydrocarbons and alcohols in the neutral lipid fraction were further separated into hydrocarbons, ketones, and alcohols using an SPE silica glass cartridge (0.5 g packing, Agilent Technologies) as described by Niemann et al. (2005).

The alcohol fractions were transformed into trimethylsilyl-derivatives by heating them at 70 °C for 1 h after the addition of 100 μl pyridine and 50 μl BSTFA. After cooling at room temperature, the excess solvent was evaporated, and the remaining TMS adducts were re-suspended in 500 μl *n*-hexane. The carboxylic acids were methylated by heating them at 60 °C for 1 h in a boron trifluouride–methanol complex. The hydrocarbons, alcohols, and polar fractions of the samples were stored at −20 °C until they underwent gas chromatography (GC), gas chromatography-mass
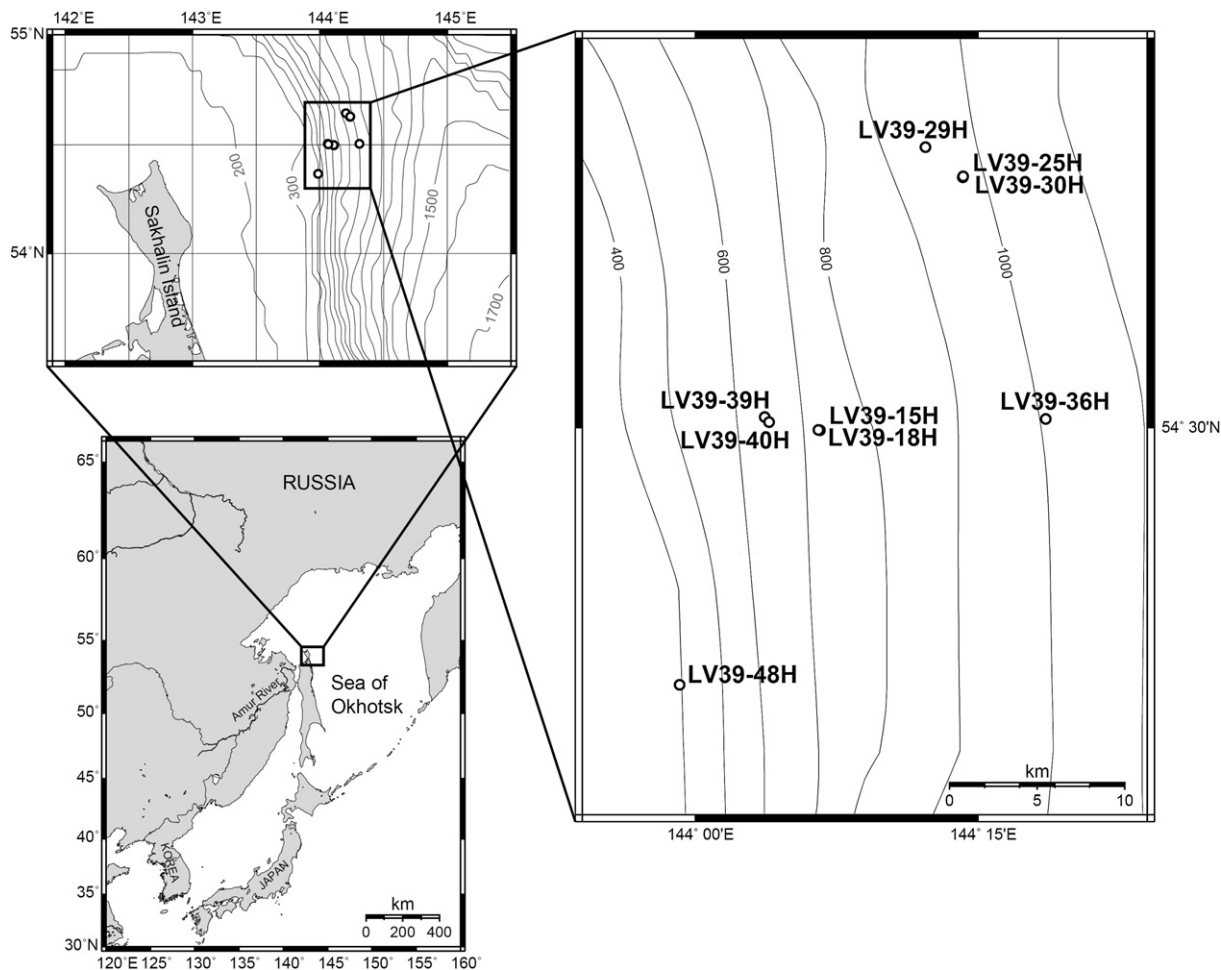
Figure 1. Geographic locations of the sediment cores collected from the Sea of Okhotsk.

spectrometry (GC–MS), and gas chromatography-isotope ratio mass spectrometry (GC-IRMS), respectively.

2.3. Preparation of dimethyl disulphide (DMDS) adducts

The double bond positions of the monoenoic fatty acids in the polar fractions were determined using DMDS adducts, according to the previously reported methods (Moss and Lambert-Fair, 1989; Nichols et al., 1986).

2.4. Gas chromatography (GC)

The analyses of the separated neutral and polar lipids were conducted using a Hewlett Packard 6890 N (Agilent Technology)

gas chromatography fitted with an apolar HP-5 fused silica, capillary column (30 m in length, 0.32 mm in internal diameter, and 0.25 μm in film thickness; J&W Scientific) and a flame ionization detector with helium as the carrier gas. The samples of the neutral lipids were injected at 60 °C with a 1-min hold time, and then the oven temperature was raised to 150 °C at a rate of 10 °C/min, then to 310 °C at a rate of 4 °C/min, and finally kept at 310 °C for 50 min. The samples of polar lipids were injected at 60 °C with a 1-min hold time and then the oven temperature was raised to 150 °C at a rate of 10 °C/min, then to 230 °C at a rate of 2 °C/min, then to 310 °C at a rate of 5 °C/min and finally kept at 310 °C for 20 min. Quantification of each compound was performed by comparing peak areas with the internal standard (5α(H)-cholestane, n-nonadecanol and n-heneicosanoic acid).

Table 1
The geophysical and geological settings and location of the cores on the continental slope offshore of NE Sakhalin during the LV39 cruise.

Station	Latitude	Longitute	Water depth (m)	Core length (cm)	Comments	GH[a]	CC[a]
LV39-15H	54°29.909′	144°06.614′	715	365	KOPRI site		+
LV39-18H	54°29.919′	144°06.526′	715	407	KOPRI site		
LV39-25H	54°37.719′	144°14.198′	880	270	Soloviev Structure site	+	+
LV39-29H	54°38.648′	144°12.218′	935	60	Canyon on the north site		
LV39-30H	54°37.743′	144°14.223′	880	320	Soloviev Structure site		
LV39-36H	54°30.265′	144°18.593′	980	237	New Structure		
LV39-39H	54°30.321′	144°03.691′	670	390	POI		
LV39-40H	54°30.162′	144°03.922′	670	260	POI	+	+
LV39-48H	54°22.029′	143°59.163′	385	55	GIZELLA		

[a] GH, gas hydrates; CC, carbonate concretions; +, occurrence of gas hydrates or carbonate concretions.

Figure 2. Gas hydrate-containing sediments recovered in the LV39-40H core.

2.5. Gas chromatography-mass spectrometry (GC−MS)

The hydrocarbons, alcohols, and carboxylic acids were identified using GC−MS (Shimadzu; GCMS-QP2010) in electron impact (EI) mode at 70 eV (cycle time 0.9 s, resolution 1000). The full scan mass spectra were recorded from m/z 40 to 800 for the alcohols, m/z 40 to 600 for the hydrocarbons, and m/z 40 to 500 for the fatty acids. The gas chromatograph was equipped with an apolar DB-5MS fused silica, capillary column (30 m in length, 0.25 mm in internal diameter, 0.25 μm in film thickness, and 10 m DRGRD; J&W Scientific) and was subjected to the same temperature program noted above for the GC measurements. The identities of the acquired mass spectra were compared to the known standards and published data.

The crocetane fraction (F_{Cr}) of the phytane/crocetane peak was calculated using the mass spectra of the C_{20} isoprenoid peaks, as described by Bian et al. (2001).

2.6. Gas chromatography-combustion-isotope ratio mass spectrometry (GC-IR-MS)

The carbon stable isotope compositions of the hydrocarbons, alcohols, and carboxylic acids were determined using a coupled gas chromatography-combustion-isotope ratio mass spectrometry (GC-IR-MS). A combustion interface (containing a copper oxide/platinum catalyst, 850 °C) of the isotope ratio mass spectrometer (Isoprime, GV Instruments) was connected to a Hewlett Packard 6890 N (Agilent Technology) gas chromatograph equipped with an apolar HP-5 fused silica, capillary column (30 m in length, 0.32 mm in internal diameter and 0.25 μm in film thickness; J&W Scientific). The samples were subjected to the same conditions noted above for the GC measurement. Reference gas CO_2 with a known $\delta^{13}C$ value

was introduced at the beginning and end of each sample measurement, and the performance of the isotope ratio mass spectrometry was compared to the n-alkane standards of known $\delta^{13}C$ values. The isotopic ratios were reported in the conventional delta (δ) notation in units of parts per thousands (‰) relative to the Vienna-Pee Dee Belemnite (V-PDB) standard with a precision of less than ±1.0‰ for duplicate runs. The $\delta^{13}C$ values reported for the alcohols and carboxylic acids were corrected as described by Huang et al. (1995).

2.7. Bulk Elements (TOC, TN) and $\delta^{13}C_{org}$ analyses

The total organic carbon and total nitrogen contents (C/N), as well as the carbon isotopic compositions of the bulk organic matter ($\delta^{13}C_{org}$), were measured after the dissolution of the carbonates with 1M HCl, subsequent washing with distilled water, and centrifugation three times. Then, the residues were dried and ground. For the $\delta^{13}C_{org}$ analysis, approximately 15−20 mg sediment was sealed inside a small tin capsule and analyzed using a continuous-flow PDZ Europa 20/20 isotope ratio mass spectrometer combined with a PDZ Europa ANCA-GSL elemental analyzer at the Stable Isotope Facility located at the University of California, Davis. As noted above, the $\delta^{13}C_{org}$ was reported in the delta (δ) notation relative to the Pee Dee Belemnite (PDB) standard, with a precision of less than ±0.2‰ for duplicate runs.

3. Results

Figure 3 presents the spatial distributions of the C/N ratios and the $\delta^{13}C_{org}$, H/L and CPI values of the sediment in the Derugin Basin within a core depth of 10 cmbsf. The C/N ratios and $\delta^{13}C_{org}$ values of the majority of the surface sediment samples indicate that the
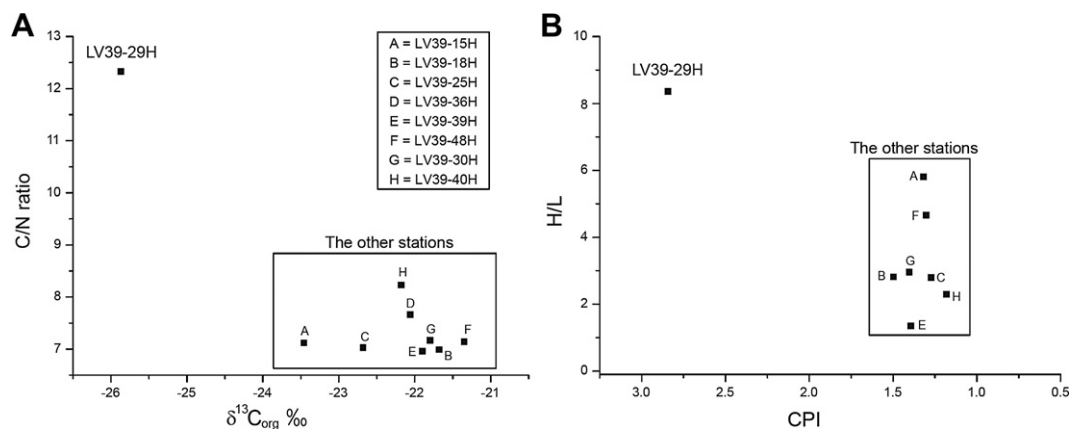

Figure 3. Crossplots of C/N ratios versus δ^{13}Corg (A) and H/L ratios versus the CPI values (B) of sediments up to 10 cmbsf core depth in the Sea of Okhotsk. The LV39-36H is not noted in Figure 3B on account of no detection of short chain n-alkanes (nC_{17}, nC_{19}).

Table 2
Concentrations (µg g^{-1} sediment dry weight) and δ^{13}C values (‰) of individual neutral lipids including n-alkanes and archaeal biomarkers within the surface sediments of the other stations.

	LV39-15H	LV39-18H	LV39-25H	LV39-29H	LV39-36H	LV39-39H	LV39-48H
	cmbsf						
	0–10	0–10	0–10	0–10	0–10	0–10	0–10
Hydrocarbons							
nC$_{12}$	0.13 (–[f])	0.26 (–)	0.18 (–)	0.14 (–)	0.13 (–)	0.19 (–26.0)	0.08 (–)
nC$_{13}$	0.10 (–)	0.17 (–31.8)	0.13 (–)	0.12 (–)	0.15 (–)	0.13 (–32.8)	0.05 (–)
nC$_{14}$	0.16 (–)	0.39 (–)	0.21 (–)	0.23 (–)	– (–)	0.27 (–27.2)	0.10 (–)
nC$_{15}$	0.18 (–)	0.33 (–)	0.18 (–)	0.20 (–)	0.12 (–)	0.58 (–34.3)	0.10 (–)
nC$_{16}$	0.17 (–)	0.25 (–)	0.19 (–)	0.18 (–)	– (–)	0.30 (–20.6)	0.09 (–)
nC$_{17}$	0.22 (–)	0.23 (–)	0.20 (–)	0.24 (–)	– (–)	0.64 (–29.9)	0.12 (–)
nC$_{18}$	0.15 (–)	0.26 (–)	0.17 (–)	0.22 (–)	– (–)	0.35 (–)	0.08 (–)
nC$_{19}$	0.16 (–)	0.14 (–)	0.17 (–)	0.32 (–26.5)	– (–)	0.18 (–)	0.11 (–)
nC$_{20}$	0.20 (–)	0.22 (–)	0.19 (–)	0.34 (–32.9)	0.13 (–)	0.33 (–)	0.09 (–)
nC$_{21}$	0.23 (–)	0.19 (–)	0.19 (–)	0.66 (–32.4)	0.23 (–)	0.20 (–)	– (–)
nC$_{22}$	0.27 (–)	0.31 (–)	0.35 (–)	0.65 (–32.4)	0.41 (–28.7)	0.30 (–)	0.14 (–)
nC$_{23}$	0.31 (–)	0.43 (–29.1)	0.44 (–26.8)	1.49 (–30.6)	0.94 (–30.0)	0.35 (–)	0.14 (–)
nC$_{24}$	0.31 (–)	0.34 (–)	0.40 (–31.0)	0.77 (–32.8)	0.58 (–31.6)	0.38 (–)	0.15 (–)
nC$_{25}$	0.46 (–31.5)	0.50 (–28.9)	0.50 (–28.0)	1.43 (–31.7)	0.89 (–32.1)	0.38 (–)	0.17 (–)
nC$_{26}$	0.47 (–29.6)	0.39 (–31.1)	0.48 (–29.1)	0.71 (–32.1)	1.14 (–31.6)	0.35 (–)	0.17 (–)
nC$_{27}$	0.83 (–30.5)	0.61 (–30.6)	0.56 (–28.3)	2.45 (–31.6)	1.77 (–30.6)	0.56 (–32.2)	0.26 (–31.4)
nC$_{28}$	0.83 (–29.5)	0.42 (–29.0)	0.40 (–30.8)	0.65 (–31.8)	1.98 (–30.2)	0.39 (–32.9)	0.22 (–30.1)
nC$_{29}$	1.21 (–30.1)	0.69 (–31.8)	0.49 (–28.5)	2.00 (–31.9)	2.47 (–30.1)	0.67 (–31.1)	0.28 (–26.8)
nC$_{30}$	0.98 (–30.7)	0.45 (–24.8)	0.34 (–)	0.55 (–30.4)	0.29 (–29.6)	0.43 (–29.5)	0.23 (–31.2)
nC$_{31}$	1.21 (–29.7)	0.69 (–29.0)	0.46 (–26.3)	1.87 (–31.5)	3.82 (–20.9)	0.66 (–29.7)	0.23 (–31.8)
nC$_{32}$	0.64 (–31.3)	0.39 (–)	0.27 (–)	0.48 (–29.9)	1.35 (–29.8)	0.37 (–)	0.17 (–)
nC$_{33}$	0.55 (–30.3)	0.40 (–)	0.30 (–)	0.70 (–31.9)	1.05 (–32.4)	0.40 (–)	0.15 (–)
nC$_{34}$	0.39 (–)	0.32 (–)	0.23 (–)	0.25 (–)	0.79 (–31.9)	0.31 (–)	0.12 (–)
nC$_{35}$	0.28 (–)	0.27 (–)	0.35 (–)	0.27 (–)	0.63 (–30.6)	0.33 (–)	0.16 (–)
nC$_{36}$	– (–)	– (–)	– (–)	– (–)	– (–)	– (–)	– (–)
nC$_{37}$	– (–)	– (–)	– (–)	– (–)	0.32 (–)	– (–)	– (–)
nC$_{38}$	– (–)	– (–)	– (–)	– (–)	0.31 (–)	– (–)	– (–)
nC$_{39}$	– (–)	– (–)	– (–)	– (–)	0.28 (–)	– (–)	– (–)
nC$_{40}$	– (–)	– (–)	– (–)	– (–)	0.29 (–)	– (–)	– (–)
Crocetane	– (–)	– (–)	– (–)	– (–)	– (–)	– (–)	– (–)
PMI[b]	– (–)	– (–)	– (–)	– (–)	– (–)	– (–)	– (–)
$\sum$ n-alkanes (C$_{12}$–C$_{40}$)	10.44	8.66	7.36	16.93	20.05	9.05	3.43
CPI[c]	1.32	1.50	1.27	2.84	2.04	1.39	1.18
H/L[d]	5.80	2.82	2.79	8.36	NC	1.35	2.30
Alcohols							
archaeol	1.31 (–117.5)	– (–)	0.88 (–)	1.06 (–130.6)	0.79 (–)	0.90 (–)	– (–)
sn–2–hydroxyarchaeol	2.22 (–123.3)	– (–)	0.96 (–)	0.99 (–)	0.87 (–)	1.00 (–)	– (–)
OH-Ar-index[e]	1.70	NC[a]	1.10	0.94	1.11	1.11	NC

[a] NC, not calculated.
[b] PMI = 2,6,10,15,19-pentamethylicosane.
[c] CPI = 2($\sum$Odd nC$_{23}$ to nC$_{31}$)/[($\sum$Even nC$_{22}$ to nC$_{30}$) + ($\sum$Even nC$_{24}$ to nC$_{32}$)] (Saito and Suzuki, 2007).
[d] H/L = (nC$_{27}$ + nC$_{29}$ + nC$_{31}$)/(nC$_{15}$ + nC$_{17}$ + nC$_{19}$) (Bourbonniere and Meyers, 1996).
[e] OH-Ar-index = sn-2-hydroxyarchaeol/archaeol (Blumenberg et al., 2004).
[f] not detected.

sedimentary organic matter is composed of marine algal-derived organic matter typically. However, the sediment sample from the LV39-29H station had a particularly high C/N ratio and ^{13}C-depleted values compared to the other stations, indicating terrigenous, vascular land plant-derived organic matter input (Fig. 3A). This result is also coinciding with the higher CPI (2.84) and H/L (8.36) values in the sediment at the LV39-29H station than in sediments from other stations (Fig. 3B).

The sum of individual n-alkanes (nC$_{12}$ − nC$_{40}$) concentrations ranged from 3.43 to 20.05 µg gdw^{-1} demonstrating approximately similar composition among the stations (Table 2). However, no crocetane and PMI as the typical biomarker compounds of methanotrophic archaea were detected within the 10 cm core sediments at all stations, and only archaeal biomarkers such as archaeol and sn-2-hydroxyarchaeol were found in the surface sediment at six stations except LV39-18H, LV39-30H and LV39-48H (Table 2 and Table 4). Also, some biomarker compounds (iso- and anteiso- C$_{15:0}$ and C$_{16:1\omega5}$) sulphate reduction bacteria among the individual carboxylic acids were detected at all stations except LV39-40H (Table 3 and Table 6).

The δ^{13}C values of individual n-alkanes (nC$_{12}$ − nC$_{40}$) and carboxylic acids ranged from −21.0 to −36.6‰ in the 10 cm depth of surface sediment at all stations, but quite low value (−88.5‰) of C$_{16:1\omega5}$ was found at a station (LV39-15H), providing a strong indication of sulphate reduction biomarker (Tables 2, 3 and 7). In addition, archaeol and sn-2-hydroxyarchaeol showed extremely lighter values (−117.5 to −130.6‰) as the obvious AOM biomarkers at LV39-15H and LV39-29H (Table 2).

The depth profiles of the C/N ratios and contents, δ^{13}C$_{org}$ values of TOC, H/L ratios, and CPI values of two selected sediment cores were also compared in order to identify the origin of the vertically distributed organic matter (Fig. 4). The average TOC concentrations of the samples in the LV39-30H and LV39-40H cores were 1.19% and 1.34%, respectively. Although the C/N and H/L ratios within the range of 110–130 cmbsf in the LV39-30H cores exhibited a small negative shift, the general range of the C/N and H/L ratios indicated that the input of terrestrial organic matter was insignificant. The CPI and δ^{13}C$_{org}$ ranges were within the typical range for marine organic matter (Fig. 4A). In contrast to the results for the LV39-30H

Table 3
Concentrations (µg g^{-1} sediment dry weight) and δ^{13}C values (‰) of individual carboxylic acids, including bacterial biomarkers, within the surface sediments of the other stations.

	LV39-15H	LV39-18H	LV39-25H	LV39-29H	LV39-36H	LV39-39H	LV39-48H
	cmbsf						
	0–10	0–10	0–10	0–10	0–10	0–10	0–10
$C_{11:0}$	$-^e$ (−)	− (−)	− (−)	− (−)	0.95 (−)	− (−)	− (−)
$C_{12:0}$	1.09 (−)	1.04 (−)	0.97 (−)	1.06 (−)	1.06 (−)	1.05 (−)	0.62 (−)
$C_{13:0}$	0.98 (−)	0.98 (−)	− (−)	1.00 (−)	0.97 (−)	0.97 (−)	− (−)
$C_{14:0}$	1.09 (−36.6)	1.83 (−25.3)	1.28 (−26.9)	1.78 (−25.0)	1.36 (−24.7)	1.14 (−25.4)	0.65 (−)
i-$C_{15:0}$	1.14 (−)	1.22 (−23.9)	1.07 (−)	1.06 (−)	1.25 (−22.3)	1.19 (−)	0.65 (−)
a-$C_{15:0}$	0.28 (−)	0.32 (−29.5)	0.41 (−)	0.32 (−)	0.28 (−25.6)	0.25 (−)	0.15 (−)
$C_{15:0}$	0.80 (−)	1.00 (−24.4)	0.79 (−)	0.95 (−26.9)	0.82 (−)	0.95 (−)	0.46 (−)
i-$C_{16:0}$	0.70 (−)	0.73 (−)	0.72 (−)	0.72 (−)	0.71 (−)	0.70 (−)	0.42 (−)
$C_{16:1\omega5}$	1.00 (−88.5)	0.99 (−)	0.89 (−)	0.67 (−)	0.82 (−)	0.92 (−)	0.41 (−)
$C_{16:1\omega7}$	0.79 (−)	2.36 (−25.4)	1.21 (−32.0)	0.73 (−)	1.48 (−24.9)	1.08 (−)	0.44 (−)
$C_{16:0}$	2.52 (−27.3)	4.76 (−25.2)	2.57 (−26.9)	4.05 (−29.5)	3.70 (−26.2)	5.94 (−27.7)	0.85 (−24.4)
i-$C_{17:0}$	0.77 (−)	0.81 (−)	0.72 (−)	0.65 (−)	0.75 (−)	0.67 (−)	0.43 (−)
$C_{17:0}$	0.74 (−)	0.74 (−)	0.63 (−)	0.74 (−)	0.65 (−)	0.74 (−)	0.36 (−)
$C_{18:2\omega6}$	− (−)	0.09 (−)	0.04 (−)	0.03 (−)	0.18 (−)	0.03 (−)	− (−)
$C_{18:1\omega9c}$	2.14 (−)	2.53 (−24.6)	2.22 (−29.3)	2.27 (−27.3)	2.80 (−21.2)	2.32 (−)	1.28 (−)
$C_{18:1\omega9t}$	0.86 (−)	1.23 (−25.7)	0.95 (−)	0.82 (−)	1.30 (−21.0)	1.18 (−)	0.44 (−)
$C_{18:0}$	1.46 (−27.3)	1.68 (−27.1)	1.28 (−27.4)	3.25 (−30.0)	1.58 (−24.2)	21.82 (−29.7)	0.60 (−26.6)
$C_{20:0}$	0.85 (−)	1.14 (−33.9)	0.93 (−)	4.47 (−32.8)	0.94 (−29.7)	1.07 (−)	0.46 (−)
$\sum$ NSats[a]	9.53	13.17	8.44	17.30	12.02	33.68	3.99
$\sum$ Monos[b]	4.80	7.12	5.27	4.50	6.40	5.50	2.57
$\sum$ BrSat[c]	2.89	3.08	2.92	2.75	2.99	2.82	1.66
$\sum$ SRB[d]	2.41	2.53	2.37	2.05	2.35	2.36	1.22
a-$C_{15:0}$/i-$C_{15:0}$	0.24	0.26	0.38	0.30	0.23	0.21	0.23
$C_{16:1\omega5}$/i-$C_{15:0}$	0.88	0.82	0.83	0.63	0.66	0.77	0.63
$C_{18:1\omega9t}$/$C_{18:1\omega9c}$	0.40	0.49	0.43	0.36	0.47	0.51	0.34

[a] NSats, saturated straight chain fatty acids.
[b] Monos, monounsaturated fatty acids.
[c] BrSat, branched fatty acids.
[d] SRB, i-$C_{15:0}$ + a-$C_{15:0}$ + $C_{16:1\omega5}$.
[e] not detected.

cores, the C/N ratios increased with depth until approximately 110 cmbsf in the LV39-40H cores (Fig. 4B). The change of C/N ratios in the LV39-40H cores was a result of the preferential degradation of buried organic nitrogen during early diagenesis in a stable sedimentation environment (Aiken et al., 1985). The H/L values in the core were ranged from 1.90 to 8.28 with relatively low CPI values (close to 1.0).

Archaeal-specific lipid biomarkers, including sn-2-hydroxyarchaeol and archaeol for Archaea, were only detected in the LV39-40H core and with extremely low δ^{13}C values ranging from −122.7‰ to −47.7‰ (Table 5 and Fig. 6). The stable carbon isotope ratios of most of sulphate reduction bacterial biomarkers (iso- and anteiso- $C_{15:0}$ and $C_{16:1\omega5}$) were not detected due to their low concentrations, except at the 10 cm depth of surface sediment of LV39-30H). Saturated fatty acids, including $C_{16:0}$ and $C_{18:0}$ in the LV39-40H and LV39-30H cores, were found in distinctively high concentrations in accordance with a slight concomitant decrease in the δ^{13}C signals at sediment depths of 150–160 cmbsf (Fig. 5).

Interestingly, the δ^{13}C$_{org}$ of the sediment at 90 to100 cmbsf in the LV39-40H cores showed a negative anomaly with a different carbon isotopic value (Δδ^{13}C$_{org}$ = 2.5‰) than the background trend (Fig. 4B).

4. Discussion

4.1. Characteristics and origin of organic matter in surface sediments

The atomic C/N ratios and δ^{13}C$_{org}$ values have been broadly utilized in order to determine the origin of sedimentary organic matter derived from marine algae versus terrestrial, vascular plants (Prahl et al., 1980; Premuzic et al., 1982; Ishiwatari and Uzaki, 1987; Jasper and Gagosian, 1990; Meyers et al., 1996). Marine-algal derived organic matter typically has C/N ratios of 4–9, while terrigenous, vascular land plant-derived organic matter has higher values than 20 (Krishnamurthy et al., 1986; Emerson and Hedges, 1988; Mayer, 1994). Similarly, the organic matter produced from atmospheric CO$_2$ (δ^{13}C = −8‰; Keeling et al., 1995) through the C$_3$ pathway by terrestrial plants, including most trees and shrubs, generally has a δ^{13}C range of −32‰ to −21‰ (average = ca. −27‰; Deines, 1980). In contrast, marine organic matter produced by marine algae from dissolved bicarbonate (δ^{13}C = 0‰; Jasper and Gagosian, 1990; Mayer, 1994) has a typical δ^{13}C range of −23 to −16‰ (average = ca. −19‰; Deines, 1980). In addition, the organic matter produced by plants, such as tropical savannah grasses and sedges, through the C$_4$ pathway has a δ^{13}C range of −17‰ to −9‰ (average = ca. −14‰; Deines, 1980).

Similarly, the terrigenous to aquatic ratio (H/L) and the carbon preference index (CPI) based on the odd/even ratio of the individual n-alkanes have also been widely used to identify sedimentary organic matter (Bray and Evans, 1961; Eglinton and Hamilton, 1967; McCaffrey et al., 1991; Jasper and Gagosian, 1993; Bourbonniere and Meyers, 1996). The odd-numbered long-chain hydrocarbons within the range of nC$_{21}$ to nC$_{35}$, which are synthesized by higher terrestrial plants, such as Sphagnum sp. which is characterized by a specific n-alkane maximum value of nC$_{23}$, are major components in terrestrial organic matter (Eglinton and Hamilton, 1963; Corrigan et al., 1973; Nott et al., 2000). Bourbonniere and Meyers (1996) suggested that the H/L ratio reflects the change in the terrigenous/aquatic mixing of the hydrocarbons due to the short chain n-alkanes (nC$_{15}$–nC$_{20}$) that are primarily derived from algae and planktonic bacteria (Han and Calvin, 1969). The CPI values of the organic matter derived from vascular plant waxes are generally in the approximate range of 4–10 (Tulloch, 1976; Rieley et al., 1991),

Table 4
Concentrations (μg g^{-1} sediment dry weight) of individual neutral lipids including *n*-alkanes and archaeal biomarkers within LV39-30H and LV39-40H sediments.

	LV39-30H						LV39-40H								
	cmbsf														
	0–10	50–60	100–110	150–160	200–210	250–260	0–10	50–60	90–100	100–110	120–130	150–160	170–180	200–210	230–240
Hydrocarbons															
nC$_{12}$	0.19	0.16	0.39	0.13	0.25	0.15	0.31	0.22	0.23	0.50	0.14	0.18	0.15	0.15	0.16
nC$_{13}$	0.12	0.17	0.23	0.08	0.20	0.12	0.16	0.14	0.21	0.20	0.10	0.17	0.10	0.11	0.18
nC$_{14}$	0.17	0.21	0.35	0.17	0.37	0.17	0.39	0.24	0.29	0.62	0.17	0.25	0.23	0.16	0.24
nC$_{15}$	0.32	0.17	0.29	0.17	0.23	0.24	0.18	0.16	0.40	0.18	0.16	0.46	0.16	0.16	0.27
nC$_{16}$	0.12	0.24	0.25	0.18	0.25	0.16	0.23	0.20	0.26	0.31	0.17	0.26	0.18	0.15	0.18
nC$_{17}$	0.18	0.24	0.22	0.17	0.25	0.29	0.17	0.16	0.29	0.20	0.18	0.56	0.16	0.16	0.27
nC$_{18}$	0.18	0.20	0.28	0.20	0.23	0.28	0.23	0.15	0.18	0.18	0.13	0.19	0.16	0.19	0.13
nC$_{19}$	0.12	0.13	0.19	0.15	0.22	0.19	0.17	0.14	0.13	0.14	0.15	0.16	0.15	0.17	0.13
nC$_{20}$	0.31	0.20	0.35	0.17	0.24	0.20	0.19	0.19	0.23	0.23	0.17	0.28	0.18	0.17	0.20
nC$_{21}$	0.19	0.18	0.52	0.17	0.23	0.24	0.22	0.18	0.19	0.30	0.17	0.19	0.17	0.17	0.20
nC$_{22}$	0.31	0.27	0.79	0.26	0.37	0.30	0.38	0.28	0.24	0.30	0.21	0.41	0.20	0.29	0.33
nC$_{23}$	0.34	0.30	1.60	0.39	0.85	0.42	0.51	0.38	0.32	0.29	0.25	0.37	0.30	0.31	0.51
nC$_{24}$	0.35	0.34	0.62	0.26	0.43	0.32	0.44	0.38	0.32	0.32	0.19	0.41	0.19	0.27	0.37
nC$_{25}$	0.52	0.49	0.91	0.35	0.50	0.41	0.54	0.54	0.47	0.46	0.32	0.39	0.63	0.39	0.51
nC$_{26}$	0.52	0.46	0.74	0.28	0.43	0.36	0.37	0.50	0.34	0.38	0.26	0.38	0.89	0.31	0.52
nC$_{27}$	0.80	0.71	1.08	0.45	0.66	0.54	0.57	0.81	0.54	0.65	0.45	0.55	1.30	0.54	0.82
nC$_{28}$	0.73	0.89	1.06	0.36	0.52	0.39	0.37	0.69	0.38	0.63	0.28	0.42	1.20	0.32	0.83
nC$_{29}$	1.04	1.10	1.58	0.46	0.72	0.47	0.42	0.92	0.50	0.17	0.43	0.71	1.11	0.45	1.19
nC$_{30}$	0.85	1.10	1.41	0.44	0.60	0.37	0.32	0.20	0.33	0.18	0.18	0.51	1.40	0.29	0.99
nC$_{31}$	1.07	1.34	1.91	0.68	0.71	0.46	0.52	1.38	0.51	0.88	0.41	0.80	1.48	0.47	1.41
nC$_{32}$	0.56	0.63	0.80	0.35	0.44	0.32	0.26	0.44	0.27	0.51	0.26	0.39	0.85	0.23	0.67
nC$_{33}$	0.52	0.50	0.67	0.29	0.39	0.34	0.26	0.40	0.26	0.38	0.27	0.43	0.83	0.26	0.57
nC$_{34}$	0.35	0.33	0.48	0.22	0.30	0.28	0.20	0.28	0.20	0.26	0.19	0.25	0.61	0.20	0.43
nC$_{35}$	0.27	0.26	0.40	0.20	0.30	0.28	0.21	0.25	0.21	0.23	0.20	0.41	0.47	0.21	0.29
nC$_{36}$	–[f]	–	–	–	–	–	–	–	–	–	–	–	–	–	0.24
nC$_{37}$	0.21	–	0.23	–	–	–	–	0.23	0.27	–	–	–	0.22	–	0.23
nC$_{38}$	–	–	–	–	–	–	–	–	–	–	–	–	–	–	0.25
nC$_{39}$	–	–	0.25	–	–	–	–	–	–	–	–	–	–	–	–
nC$_{40}$	0.28	–	0.38	0.38	–	–	–	–	–	–	–	–	0.29	–	–
Crocetane	–	–	–	–	–	–	–	0.17	–	0.19	0.16	0.29	0.18	0.21	0.14
PMI[b]	–	–	–	–	–	–	–	–	–	–	–	–	–	–	–
$\sum$ *n*-alkanes (C$_{12}$–C$_{40}$)	10.63	10.62	17.97	6.95	9.68	7.29	7.61	9.46	7.59	8.49	5.44	9.10	13.61	6.12	12.14
CPI[c]	1.30	1.22	1.53	1.40	1.44	1.30	1.40	1.90	1.44	1.28	1.61	1.32	1.15	1.48	1.38
H/L[d]	4.65	5.89	6.50	3.25	3.01	2.04	2.96	6.75	1.90	3.28	2.63	1.75	8.28	2.99	5.12
Alcohols															
archaeol	–	–	–	–	–	–	–	0.86	1.42	0.96	NA[a]	0.87	0.89	1.14	0.83
sn–2–hydroxyarchaeol	–	–	–	–	–	–	0.77	1.10	1.73	1.04	NA	0.99	0.99	1.45	0.94
OH-Ar-index[e]	NC	NC	NC	NC	NC	NC	NC	1.27	1.21	1.08	NC	1.14	1.10	1.27	1.13

[a] NA, not analysed; NC, not calculated.
[b] PMI = 2,6,10,15,19-pentamethylicosane.
[c] CPI = 2($\sum$Odd nC$_{23}$ to nC$_{31}$)/[($\sum$Even nC$_{22}$ to nC$_{30}$)+($\sum$Even nC$_{24}$ to nC$_{32}$)] (Saito and Suzuki, 2007).
[d] H/L = (nC$_{27}$ + nC$_{29}$ + nC$_{31}$)/(nC$_{15}$ + nC$_{17}$ + nC$_{19}$) (Bourbonniere and Meyers, 1996).
[e] OH-Ar-index = *sn*-2-hydroxyarchaeol/archaeol (Blumenberg et al., 2004).
[f] not detected.

whereas the CPI values of the organic matter in marine bacteria and algae range from approximately 1.0–1.5 (Volkman et al., 1980; Nichols et al., 1988).

Seki et al. (2006) reported fluctuations in the δ^{13}C$_{org}$ values (from ca. −27‰ to −20‰) and low C/N ratios (from ca. 4 to 9) in the settling particles in the western region of the Sea of Okhotsk and suggested that the seasonal changes in the δ^{13}C$_{org}$ values might be influenced more by the algal growth rate and phytoplankton species than by the varying contributions of the marine versus terrestrial organic matter (Rau et al., 1992; Francois et al., 1993). However, the lowest δ^{13}C$_{org}$ value (−25.87‰) and highest C/N ratio (12.33) among the studied sampling sites were observed at the LV39-29H station, and these high levels were probably caused by the contribution of terrigenous organic matter. The major transportation pathways for terrigenous organic matter to the Sea of Okhotsk might include ice-rafted debris (IRD) via sea ice transport or freshwater inflow from the discharge of the Amur River (Biebow and Huetten, 1999; Lembke et al., 2003).

In addition, archaeol and *sn*-2-hydroxyarchaeol were shown at the surface 10 cm sediment of three stations (LV39-15H, LV39-29H, LV39-40H), with their extremely light carbon stable isotope ratios (Table 2). These ^{13}C-depleted archaeol and *sn*-2-hydroyarchaeol strongly suggest that these should be archaeal biomarkers related to methane in the seafloor sediments. Fingerprinting of the diagnostic ^{13}C-depleted compounds typically associated with a strong carbon isotopic fractionation during methane uptake in methanotrophic communities has been used extensively to examine the anaerobic methanotrophic organisms in the sediment samples from various, modern cold-seep environments (Hinrichs et al., 1999; Elvert et al., 2000, 2001; Thiel et al., 2001). These environments include eastern Mediterranean mud volcanoes (Pancost et al., 2000, 2001; Werne et al., 2002; Aloisi et al., 2002), ancient methane seeps (Thiel et al., 1999), and non-methane seep environments characterized by AOM, such as the water columns of the Black Sea (Schouten et al., 2001b) and the Kattegatt Strait (Bian et al., 2001). The biological, carbon isotopic fractionations during the methanotrophic and methanogenic processes occurred due to the weaker coherence of the lighter isotope (e.g., ^{12}C), relative to the heavier isotope (e.g., ^{13}C) (Hoefs, 1980; Whiticar, 1999; Elvert et al., 1999; Orphan et al., 2001).

Table 5
$\delta^{13}C$ values (‰) of individual neutral lipids including n-alkanes and archaeal biomarkers within LV39-30H and LV39-40H sediments.

	LV39-30H						LV39-40H								
	cmbsf														
	0–10	50–60	100–110	150–160	200–210	250–260	0–10	50–60	90–100	100–110	120–130	150–160	170–180	200–210	230–240
Hydrocarbons															
nC_{12}	−27.9	−21.6	−25.6	−[c]	–	–	−23.4	−27.0	−28.5	−26.8	–	−23.0	–	–	–
nC_{13}	−30.4	−29.2	−30.3	–	–	–	−30.7	−30.7	−29.9	−31.4	–	−29.0	–	–	−28.8
nC_{14}	−25.6	−26.5	−28.3	–	–	–	−28.3	−25.9	−28.1	−27.9	–	−27.9	−28.3	–	−27.6
nC_{15}	−33.8	−30.3	−34.0	–	–	–	–	–	−33.7	–	–	−34.0	–	–	−29.0
nC_{16}	–	–	−27.8	–	–	–	−25.0	−25.9	−30.0	−28.0	–	−26.2	–	–	–
nC_{17}	–	–	–	–	–	–	–	–	−33.3	–	–	−31.7	–	–	−25.6
nC_{18}	–	–	–	–	–	–	–	–	–	–	–	–	–	–	–
nC_{19}	–	–	–	–	–	–	–	–	–	–	–	–	–	–	–
nC_{20}	–	–	–	–	–	–	–	–	–	–	–	–	–	–	–
nC_{21}	–	–	–	–	–	–	–	–	–	–	–	–	–	–	–
nC_{22}	–	–	−32.1	–	–	–	–	–	–	–	–	–	–	–	–
nC_{23}	−31.2	–	−29.9	−29.8	−30.2	−32.5	−46.8	−32.6	–	–	–	−25.3	−29.8	–	−28.7
nC_{24}	−31.1	–	−30.5	–	–	–	−34.0	−31.8	–	–	–	–	−29.6	–	−33.4
nC_{25}	−27.8	−33.7	−31.6	–	–	–	−31.5	−34.1	–	−33.0	–	–	−28.4	−31.3	−32.1
nC_{26}	−26.9	−29.3	−29.2	–	–	–	−30.6	−29.0	−26.5	−28.3	–	−27.6	−27.2	–	−31.7
nC_{27}	−28.7	−29.5	−30.3	−28.6	−31.1	−30.5	−30.9	−28.7	−29.6	−31.4	−29.9	−30.5	−29.2	−31.1	−31.7
nC_{28}	−27.8	−30.0	−30.2	−28.6	−34.4	−30.0	−29.5	−29.3	−31.1	−30.4	–	−28.6	−28.0	–	−30.7
nC_{29}	−29.2	−30.3	−30.2	−27.7	−30.2	–	−32.6	−29.8	−28.3	−31.1	−29.8	−29.0	−28.3	−30.5	−30.3
nC_{30}	−29.1	−28.1	−28.1	−26.7	−30.1	–	–	−32.0	−27.3	−30.8	–	−29.7	−26.2	–	−29.2
nC_{31}	−26.5	−25.0	−26.3	−25.5	−25.9	−27.2	−31.3	−21.2	–	−28.2	−31.2	−29.0	−25.0	−31.0	−27.8
nC_{32}	−28.1	−29.3	−30.2	−31.8	–	–	–	−27.3	–	−30.6	–	−30.8	−28.3	–	−29.3
nC_{33}	−29.5	−27.2	−28.4	–	–	–	–	−30.2	–	−32.3	–	−28.0	−30.7	–	−28.1
nC_{34}	–	–	–	–	–	–	–	–	–	–	–	–	–	–	−30.1
nC_{35}	–	–	–	–	–	–	–	–	–	–	–	–	–	–	–
nC_{36}	–	–	–	–	–	–	–	–	–	–	–	–	–	–	–
nC_{37}	–	–	–	–	–	–	–	–	–	–	–	–	–	–	–
nC_{38}	–	–	–	–	–	–	–	–	–	–	–	–	–	–	–
nC_{39}	–	–	–	–	–	–	–	–	–	–	–	–	–	–	–
nC_{40}	–	–	–	–	–	–	–	–	–	–	–	–	–	–	–
Crocetane	–	–	–	–	–	–	–	–	–	–	–	–	–	–	–
PMI[b]	–	–	–	–	–	–	–	–	–	–	–	–	–	–	–
Alcohols															
archaeol	–	–	–	–	–	–	–	–	−115.6	−101.5	NA[a]	–	–	−93.2	−47.7
sn−2−hydroxyarchaeol	–	–	–	–	–	–	–	−121.6	−122.7	−104.8	NA	–	−93.5	−116.2	−87.3

[a] NA, not analysed.
[b] PMI = 2,6,10,15,19-pentamethylicosane.
[c] not detected.

In the present study, the ^{13}C- depleted archaeol and sn-2-hydroyarchaeol are consistant with extraordinary low $\delta^{13}C$ value of $C_{16:1\omega5}$ at LV39-15H as a biomarker of sulphate reduction bacteria. Terminally branched iso- and anteiso- $C_{15:0}$ fatty acids are abundant compounds in sulphate-reducing bacteria, including the common *Desulfovibrio* (Boon et al., 1977; Edlund et al., 1985; Kaneda, 1991; Vainshtein et al., 1992; Dzierzewicz et al., 1996; Feio et al., 1998). The anteiso- $C_{15:0}$ fatty acid is a prominent membrane constituent of *Desulfosarcina variabilis* and *Desulfococcus multivorans* (Kohring et al., 1994). A high $C_{16:1\omega5}$ content was also observed in the *Desulfosarcina/Desulfococcus* (DSS) cluster (Elvert et al., 2003; Orcutt et al., 2005).

In our study sites, the overall composition of the surficial sedimentary organic matter was found as derivatives of planktonic organisms (planktonic eukaryotes as well as bacteria), whereas only one core was found to contain signiciant amounts of terrigenous organic matter. Also, both lipid biomarkers of methanotrophic archaea (archaeol/sn-2-hydroxyarchaeol) and sulphate reducing bacteria fatty acid ($C_{16:1\omega5}$) were found in the surface sediment of the only station (LV39-15H) with strong ^{13}C depletions, indicating the presence of AOM in the uppermost sediment layers.

4.2. Anaerobic oxidation of methane in the methane hydrate-bearing sediments

The highest concentration of interstitial methane in the LV39-40H core is about 100 times higher than the concentration in the LV39-30H core (Fig. 4). This large methane flux in LV39-40H might be due to dissociation of methane hydrate in the sediment. The gaseous methane that continuously ascends along the faults generated by accretionary tectonics with stratified deposits most likely plays a decisive role in the occurrence of the gas hydrate in this region (Luan et al., 2008). Moreover, in three stations, authigenic carbonate precipitates were present (LV39-15H, −25H and −40H), which are further indicating that either AOM or sulphate reduction played a significant role in these sites. In cores LV39-25 and LV39-40H, apparent gas hydrate layers were identified. In the following, LV39-40H (including hydrate) and LV39-40H (no hydrate) were choosen for comparing their lipid biomarker inventory and the discussion of probable methanogenetic and methanotrophic processes.

In the present study, the concentrations and $\delta^{13}C$ values of potential lipid biomarkers for the AOM community in carboxylic acids and neutral lipids (including alcohol and hydrocarbon fractions) in two selected sediment cores were compared in order to understand the influence that gas hydrates have on the microorganism species' composition and biomass (Figs. 5 and 6). Results of archaeal-specific lipid biomarkers in the LV39-40H core with extremely low $\delta^{13}C$ values indicated that the AOM-performing archaea assimilated the methane that dissociated from the hydrate as a carbon source. Although, saturated fatty acids generally represent universal or non-specific lipids, their anomalously high concentrations and the negative excursion of the carbon

Table 6
Concentrations ($\mu g\ g^{-1}$ sediment dry weight) of individual carboxylic acids including bacterial biomarkers within LV39-30H and LV39-40H sediments.

	LV39-30H						LV39-40H							
	cmbsf													
	0–10	50–60	100–110	150–160	200–210	250–260	0–10	50–60	90–100	100–110	120–130	150–160	200–210	230–240
$C_{11:0}$	–[e]	–	–	–	–	–	–	–	–	–	–	–	–	–
$C_{12:0}$	0.90	0.97	0.90	0.93	1.41	1.34	1.19	0.92	0.96	0.92	0.99	0.95	0.94	0.93
$C_{13:0}$	0.88	0.96	–	–	–	–	–	0.91	–	–	–	–	0.93	–
$C_{14:0}$	1.42	1.45	1.20	1.31	1.39	1.44	–	1.13	1.15	1.14	1.06	1.22	1.24	1.14
$i\text{-}C_{15:0}$	1.04	1.09	0.93	0.98	1.54	1.49	–	0.99	1.02	1.00	1.03	1.04	1.00	0.96
$a\text{-}C_{15:0}$	0.73	0.25	0.32	0.33	0.53	0.41	–	0.21	0.22	0.30	0.20	0.24	0.32	0.28
$C_{15:0}$	0.76	0.79	0.72	0.75	1.13	1.13	–	0.73	0.76	0.76	0.75	0.75	0.86	0.79
$i\text{-}C_{16:0}$	0.65	0.67	0.62	0.67	0.96	0.92	–	0.64	0.65	0.65	0.67	0.65	0.66	0.66
$C_{16:1\omega5}$	0.82	0.65	0.58	0.62	1.00	0.96	–	0.64	0.68	0.64	0.71	0.63	0.69	0.67
$C_{16:1\omega7}$	1.58	0.73	0.64	0.67	1.08	1.01	1.18	0.70	0.71	0.68	0.73	0.65	0.69	0.72
$C_{16:0}$	2.80	2.72	2.32	1.93	2.44	2.33	1.72	2.04	1.98	2.27	2.13	3.76	2.40	2.19
$i\text{-}C_{17:0}$	0.64	0.68	0.59	0.64	0.95	0.93	–	0.63	0.69	0.60	0.73	0.64	0.68	0.65
$C_{17:0}$	0.54	0.59	0.53	0.55	0.86	0.84	–	0.57	0.64	0.60	0.69	0.64	0.67	0.57
$C_{18:2\omega6}$	0.13	0.04	0.04	–	0.16	0.02	–	0.01	–	–	–	–	–	0.05
$C_{18:1\omega9c}$	2.20	2.27	2.03	2.13	3.00	2.74	2.04	2.00	1.99	1.94	1.98	2.02	1.96	2.03
$C_{18:1\omega9t}$	1.24	0.88	0.84	0.80	1.04	0.93	1.21	0.73	0.74	0.75	0.72	0.86	0.71	0.77
$C_{18:0}$	1.50	2.05	1.57	1.52	1.71	1.27	0.87	1.01	0.98	1.10	1.37	15.83	1.13	1.17
$C_{20:0}$	0.96	0.92	0.82	0.77	1.09	1.05	1.31	0.89	0.83	0.94	0.87	0.89	1.00	0.92
$\sum$ NSats[a]	9.77	10.46	8.06	7.76	10.03	9.40	5.09	8.20	7.30	7.74	7.87	24.03	9.17	7.70
$\sum$ Monos[b]	5.84	4.53	4.09	4.23	6.13	5.64	4.42	4.07	4.12	4.01	4.14	4.16	4.04	4.19
$\sum$ BrSat[c]	3.06	2.70	2.46	2.62	3.99	3.76	–	2.47	2.58	2.55	2.63	2.57	2.67	2.55
$\sum$ SRB[d]	2.59	2.00	1.84	1.94	3.07	2.86	–	1.84	1.92	1.94	1.94	1.91	2.02	1.91
$a\text{-}C_{15:0}/i\text{-}C_{15:0}$	0.70	0.23	0.35	0.34	0.34	0.28	NC	0.21	0.21	0.30	0.20	0.23	0.32	0.29
$C_{16:1\omega5}/i\text{-}C_{15:0}$	0.79	0.60	0.62	0.63	0.65	0.64	NC	0.65	0.67	0.63	0.70	0.61	0.69	0.69
$C_{18:1\omega9t}/C_{18:1\omega9c}$	0.57	0.39	0.42	0.38	0.35	0.34	NC	0.36	0.37	0.39	0.36	0.42	0.36	0.38

[a] NSats, saturated straight chain fatty acids.
[b] Monos, monounsaturated fatty acids.
[c] BrSat, branched fatty acids.
[d] SRB, $i\text{-}C_{15:0} + a\text{-}C_{15:0} + C_{16:1\omega5}$.
[e] not detected; NC, not calculated.

isotopic values ($\Delta\delta^{13}C = 3\%_o$ and $7\%_o$ for $C_{16:0}$ and $C_{18:0}$, respectively) from the background trend in this study could indicate the existence of bacterial communities and the indirect assimilation of methane-derived carbon intermediate in the deep subsurface. In general, biologically produced methane has lower $\delta^{13}C$ values, in the range from $-110\%_o$ to $-60\%_o$ (for autotrophic methanogenesis) and from $-60\%_o$ to $-50\%_o$ (for acetotrophic methanogenesis), than those of thermogenic methane, which range from $-50\%_o$ to $-30\%_o$ (Sackett, 1978; Whiticar et al., 1986; Whiticar, 1999; Conrad, 2005). Therefore, the assimilation of methane produced through CO_2

reduction during AOM in marine sediments creates extremely light $\delta^{13}C$ signatures of specific lipid biomarkers (Hinrichs et al., 1999; Elvert et al., 2001; Blumenberg et al., 2004).

The anomalously negative excursion of the $\delta^{13}C_{org}$ value at 90 to 100 cmbsf in the LV39-40H cores could be a result of the incorporation of ^{13}C-depleted carbon by, for example, methane through AOM activity rather than from the contribution of terrestrial organic matter, because the other molecular characteristics (C/N, H/L, CPI ratios) are still within ranges that are typical for marine organic matter. The low carbon isotope values that were observed

Table 7
$\delta^{13}C$ values ($\%_o$) of individual carboxylic acids including bacterial biomarkers within LV39-30H and LV39-40H sediments.

|	LV39-30H						LV39-40H							
	cmbsf													
	0–10	50–60	100–110	150–160	200–210	250–260	0–10	50–60	90–100	100–110	120–130	150–160	200–210	230–240
$C_{11:0}$	–[a]	–	–	–	–	–	–	–	–	–	–	–	–	–
$C_{12:0}$	–	–	–	–	–	–	–	–	–	–	–	–	–	–
$C_{13:0}$	–	–	–	–	–	–	–	–	–	–	–	–	–	–
$C_{14:0}$	−25.7	−25.5	−21.6	−23.9	−23.6	–	–	−21.5	−27.5	−22.3	−23.5	–	−24.1	−21.2
$i\text{-}C_{15:0}$	−23.1	–	–	–	–	–	–	–	–	–	–	–	–	–
$a\text{-}C_{15:0}$	−29.6	–	–	–	–	–	–	–	–	–	–	–	–	–
$C_{15:0}$	–	–	–	–	–	–	–	–	–	–	–	–	−21.6	–
$i\text{-}C_{16:0}$	–	–	–	–	–	–	–	–	–	–	–	–	–	–
$C_{16:1\omega5}$	–	–	–	–	–	–	–	–	–	–	–	–	–	–
$C_{16:1\omega7}$	−31.0	–	–	–	–	–	−20.6	–	–	–	–	–	–	–
$C_{16:0}$	−27.1	−24.6	−24.5	−25.2	−24.8	−24.9	−24.7	−24.6	−23.2	−25.7	−24.9	−28.7	−24.2	−24.2
$i\text{-}C_{17:0}$	–	–	–	–	–	–	–	–	–	–	–	–	–	–
$C_{17:0}$	–	–	–	–	–	–	–	–	–	–	–	–	–	–
$C_{18:2\omega6}$	–	–	–	–	–	–	–	–	–	–	–	–	–	–
$C_{18:1\omega9c}$	−29.1	−25.6	−23.4	−21.7	–	–	–	–	–	–	–	–	–	–
$C_{18:1\omega9t}$	−28.2	–	–	–	–	–	–	–	–	–	–	–	–	–
$C_{18:0}$	−27.4	−24.7	−22.9	−24.8	−27.8	−26.4	–	−26.4	−24.2	−23.2	−26.9	−30.1	−26.7	−25.3
$C_{20:0}$	−30.8	−27.7	−28.3	–	–	–	–	−26.8	−30.4	−31.9	−31.2	–	−28.6	−23.8

[a] not detected.
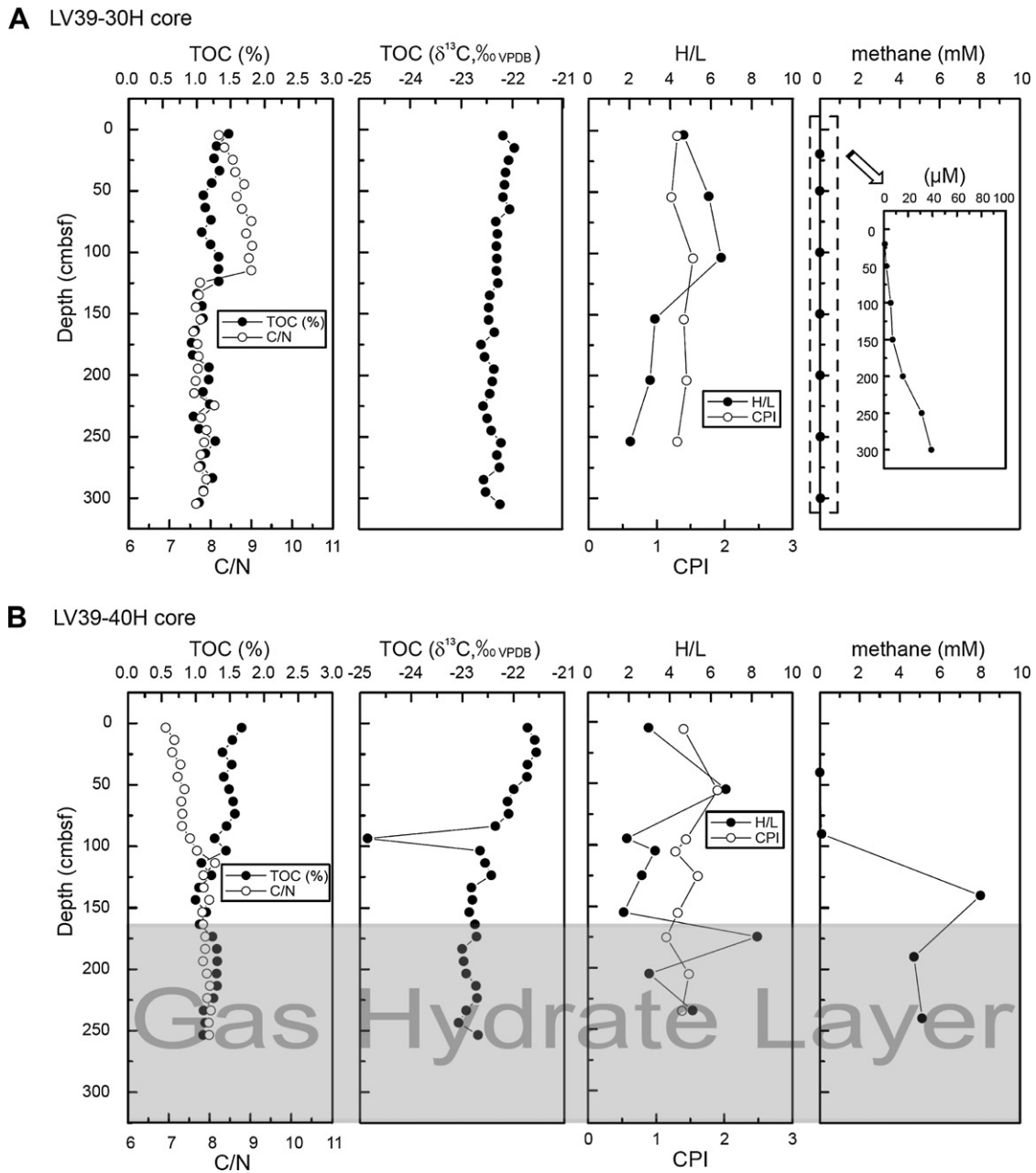
Figure 4. Depth profiles of the C/N ratios, contents, and $\delta^{13}C$ values of the TOC, H/L, CPI values and interstitial methane concentrations in the sediment core containing distinctive layers of gas hydrates (grey-shaded areas; B) and those sediment cores not containing these layers (A). The methane concentrations were obtained from Jin et al. (2007).

in the bulk organic matter have also been observed in various cold seep and mud volcano environments, which indicates that these low levels could be an indication of potential AOM consortia (Haese et al., 2003; Werne et al., 2004; Elvert et al., 2005). That assumption can be made due to the fact that the methane-derived carbon in the AOM biomass has extremely low $\delta^{13}C_{org}$ values, as compared to those of marine planktonic organic matter.

The concentrations of the two archaeal compounds, sn-2-hydroxyarchaeol and archaeol, peaked at a depth of 90–100 cmbsf in the LV39-40H cores, which was in good agreement with the negative $\delta^{13}C_{org}$ values at the same depth. The amount of AOM-derived biomass carbon was calculated by using a stable isotope mass balance equation between the bulk organic carbon and alcohol lipid biomarkers. The isotope mass balance equation is as follows.

$$\delta^{13}C_{AOM}x + (1-x)\delta^{13}C_{BG} = \delta^{13}C_{obs} \text{ (Haese et al., 2003)}$$

Where $\delta^{13}C_{AOM}$, $\delta^{13}C_{BG}$, and $\delta^{13}C_{obs}$ represent the isotopic compositions of the AOM consortium, bulk organic carbon background and bulk organic carbon at the depth of AOM. The $\times$ means contribution of AOM consortium to bulk organic carbon pool. Because the somewhat lower (by about -10 to $-20‰$) $\delta^{13}C$ values of the archaeal lipids compared with the total cell carbon determined in previous observations of isotopic compositions of individual lipids versus biomass of *Methanosarcina barkeri* grown on trimethylamine (Summons et al., 1998; Orphan et al., 2001), it is possible to infer that the range of $\delta^{13}C_{methane}$ is from $-95.6‰$ to $-112.7‰$ with the $\delta^{13}C$ values of archaeal lipids at the depth. As a result, the isotopic mass balance calculation provided that approximately 2.77–3.41% of the total organic carbon (or 0.036–0.044% dry weight sediment) was additionally bound to the
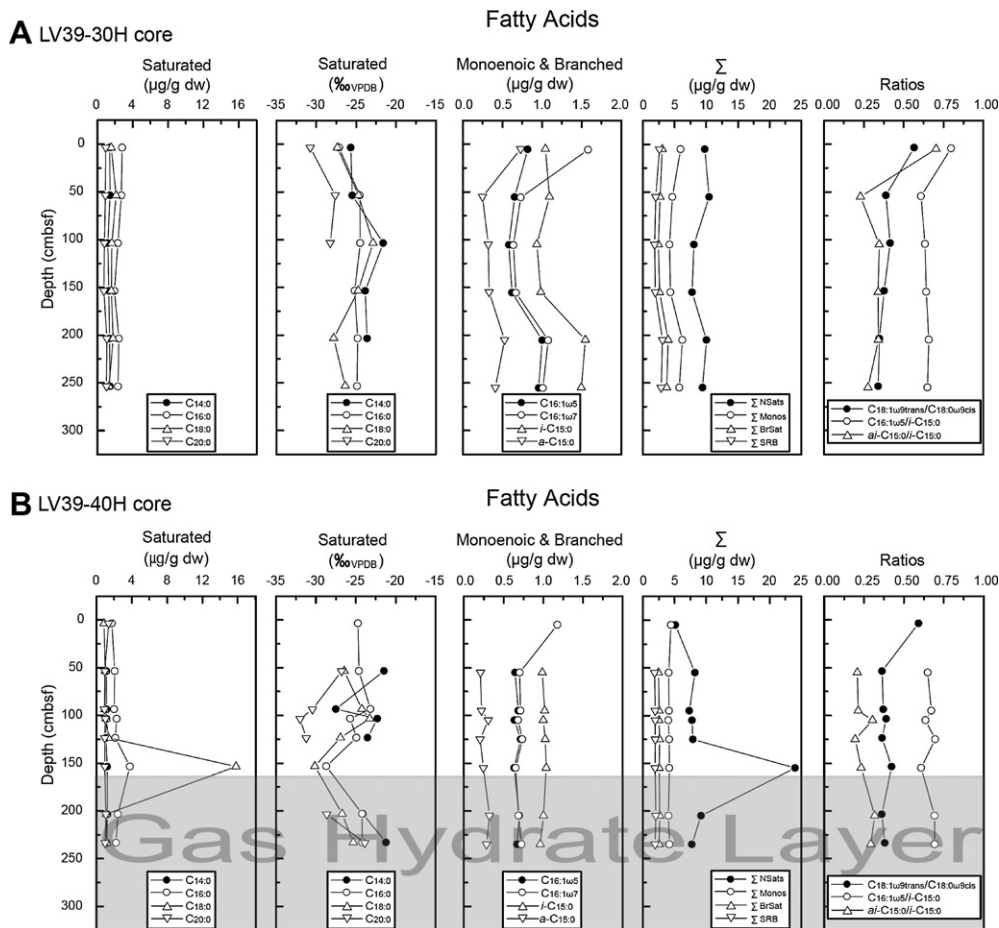
Figure 5. Depth profiles of the concentrations and $\delta^{13}C$ values of individual carboxylic acids, ratios, and sums of different types of carboxylic acids in the sediment core containing distinctive layers of gas hydrates (grey-shaded areas; B) and those sediment cores not containing these layers (A).

biomass of the microbial consortium that was responsible for the AOM within the sediment depth of 90–100 cmbsf in the LV39-40H core (Haese et al., 2003; Werne et al., 2004; Elvert et al., 2005).

On the other hand, pressure incubation using Hydrate Ridge sediments yielded 23 mg biomass carbon for the consortia, which corresponded to 0.7 mg $C_{16:1\omega5}$ fatty acid (Nauhaus et al., 2007). This quantitative relationship ($C_{16:1\omega5}$ fatty acid/biomass carbon; 3.04%) indicates that the concentration of the methanotrophic consortia biomass can be 22.3 μg C gdw^{-1} at the sediment depth of 90–100 cmbsf in the LV39-40H cores, using the $C_{16:1\omega5}$ fatty acid concentration (0.68 μg gdw^{-1}) which was measured at the same depth. The quantity of lipid biomarkers for the AOM-performing archaea at this depth does not appear to be inadequate in order to explain the extraordinarily low $\delta^{13}C_{org}$ value. Therefore, it can be deduced from the contributions of considerable quantities of ^{13}C-depleted lipids that other high molecular weight compounds, such as proteins and carbohydrates containing methane-derived carbon, are components of the viable AOM consortia in the bulk organic carbon pool at the same depth. Considering that only 0.25–1.3% of the consumed methane was directly incorporated into the biomass of the AOM consortia, while approximately 98% of the consumed methane was oxidized to CO_2 in different cold seep sites, (Nauhaus et al., 2007; Wegener et al., 2008), it can also be assumed that the assimilation of this ^{13}C-depleted CO_2 produced by the methane-oxidizing archaea could represent negative values of the organic carbon isotope. As a result, the negative carbon isotopic change in the bulk organic matter in the LV39-40H cores may be imprinted on the organic matter through the AOM process over long periods of time.

Previous studies have used the positive correlations between specific biomarkers and AOM-consortia calculations (Elvert et al., 2003, 2005; Nauhaus et al., 2007) to overcome the estimation problems for the integrated biomass carbon of the consortia and the number of archaeal or bacterial cells related to the extremely slow growth rate due to the environmental and physiological conditions (Girguis et al., 2003; Nauhaus et al., 2005). The estimated amounts of specific biomarkers in previous studies ranged from 0.62 to 0.90 × 10^{-15} g for sn-2-hydroxyarchaeol, 0.22 to 0.30 × 10^{-15} g for archaeol per ANME-2 cell, from 0.46 to 0.58 × 10^{-15} g for $C_{16:1\omega5}$, and 0.10 to 0.14 × 10^{-15} g for cyC$_{17:1\omega5,6}$ per DSS cell (Elvert et al., 2003, 2005). Using the reported ratios of specific lipid contents per AOM cell, the presumed cell numbers within the depth range of 90–100 cmbsf in the LV39-40H cores were estimated to be in the range of 1.92–6.45 × 10^9 and 1.17 to 1.48 × 10^9 for the ANME archaea (sn-2-hydroxyarchaeol, archaeol) and DSS cluster ($C_{16:1\omega5}$, cyC$_{17:1\omega5,6}$), respectively. However, these estimates are only rough approximations, because the relative amounts of biomass carbon and lipids per microbial cell may vary among different populations and environmental conditions.

4.3. Methanogenesis and classification of specific AOM consortia in methane hydrates-bearing sediments

In general, autotrophic methanogenesis is an important pathway in marine sediments underlying the zone of sulphate reduction, while acetate fermentation generates the majority of the

methane in freshwater sediments (Woltemate et al., 1984; Whiticar et al., 1986; Whiticar, 1999).

In this study, similarly, the heavy $\delta^{13}C$ values of the archaeol ($-47.7‰$) at a depth of 230–240 cmbsf in the hydrate zone of the LV39-40H cores were close to the isotopic values of the archaeol from methanogenic sources obtained from other environmental deposits (between $-17‰$ and $-34‰$) (Bolle et al., 2000; Schouten et al., 2001a). Therefore, the archaeol detected at this depth was most likely derived from both methanogenic and methanotrophic archaea. The question is if AOM is working in the deeper zone of core LV39-40H today, or if the former AOM signature is overprinted by a younger activity of methanogenic archaea. The actual AOM is around 100 cm depth in LV39-40H core, whereas the zone of methanogenesis is identified at 170–230 cm depth. The "old AOM" signature is consequently isotopically heavier than those in the "modern AOM" zone, where so far methanogenesis did not occur. The contributions of the methane produced in the hydrate zone to the formation of hydrates and to supporting methane-oxidizing populations have been also observed in previous studies (Wellsbury et al., 1997; Suess et al., 1999; Fehn et al., 2000; Valentine, 2002; Haeckel et al., 2004). In addition, the methane oxidation rates peaked in the hydrate zone sediments from the Cascadia Margin in the eastern Pacific, and the methanogenesis rates increased dramatically just below the gas hydrate stability zone (Cragg et al., 1996). These findings supported the hypothesis that the methane in deep submarine hydrates can originate in the sediments below the hydrates and support methane-oxidizing populations.

On the other hand, previous publications revealed that the ratios of specific lipid biomarkers can be used to verify the predominance of phylogenetically different clades of ANME -1, -2, and -3, as well as sulphate reducing bacterial groups (DSS, DBB) (Elvert et al., 2003; Blumenberg et al., 2004; Niemann, 2005; Niemann et al., 2006a; Nauhaus et al., 2007; Niemann and Elvert, 2008). ANME-1 archaea are characterized by a sn-2-hydroxyarchaeol to archaeol range ratio between 0 and 0.8, while those environments dominated by ANME-2 archaea and ANME-3 (2.4) are characterized by ratios between 1.1 and 5.5 (Niemann, 2005; Niemann et al., 2006a; Nauhaus et al., 2007). The presence of crocetane was also an obvious biomarker for ANME-2 (Elvert et al., 1999; Boetius et al., 2000; Blumenberg et al., 2004; Niemann and Elvert, 2008). The

magnitude of the stable carbon isotope fractionation of archaeol relative to the source methane was different for the ANME-1 dominated systems ($\Delta\delta^{13}C$ = from $-53‰$ to $-12‰$) and the ANME-2 and -3 dominated systems ($\Delta\delta^{13}C$ = from $-62‰$ to $-34‰$) (Hinrichs et al., 1999; Boetius et al., 2000; Elvert et al., 2001; Orphan et al., 2002; Teske et al., 2002; Blumenberg et al., 2004; Niemann et al., 2005; Niemann and Elvert, 2008). Similar to the use of the sn-2-hydroxyarchaeol/archaeol ratio as an archaeal fingerprint, the DSS associated with ANME-1 was also characterized by higher values of ai-$C_{15:0}/i$-$C_{15:0}$ (ca. 3.0) and lower values of $C_{16:1\omega5}/i$-$C_{15:0}$ (ca. 0.5) than the values of ai-$C_{15:0}/i$-$C_{15:0}$ (ca. 1.6) and $C_{16:1\omega5}/i$-$C_{15:0}$ (ca. 4.8) in the DSS associated with ANME-2 (Elvert et al., 2003, 2005; Blumenberg et al., 2004; Niemann and Elvert, 2008). High amounts of $C_{17:1\omega6c}$ were also observed in the DBB systems associated with ANME-3 from other SRB dominated environments (Parkes and Calder, 1985; Niemann et al., 2006a).

The stable hydrogen and carbon isotope compositions of the methane encaged in the hydrate molecules in the LV39-40H cores exhibited the typical range of microbial carbonate reduction (A. Hachikubo, personal communication). It is possible to infer that the $\delta^{13}C$ of the interstitial methane is about $-64‰$, because there is no kinetic carbon isotopic fractionation during the formation and dissociation of gas hydrates (Hachikubo et al., 2007). The stable carbon isotope fractionations of the archaeol relative to the source methane in the LV39-40H cores, which were calculated with the presumed $\delta^{13}C$ values of the interstitial methane, were different in the above layer ($\Delta\delta^{13}C$ = from $-58‰$ to $-37‰$) than in the hydrate layers ($\Delta\delta^{13}C$ = from $-29‰$ to $16‰$). The ratios of sn-2-hydroxyarchaeol/archaeol (1.08–1.27), ai-$C_{15:0}/i$-$C_{15:0}$ (0.20–0.32) and $C_{16:1\omega5}/i$-$C_{15:0}$ (0.61–0.70) showed insignificant variation throughout the core depth, indicating that the compositions of the AOM communities remained constant with depth (Figs. 5 and 6).

Although the ratios of sn-2-hydroxyarchaeol/archaeol overlapped between the range of two ANME-1 and -2 ecotypes, as a more useful index for discriminating between SRB species (Niemann and Elvert, 2008), the $C_{16:1\omega5}/i$-$C_{15:0}$ values were close to the range of the SRB which was physiologically related to the ANME-1/DSS aggregates. The results of this study indicated that the marked discrepancy in the isotopic fractionations of the archaeol throughout the sediment depth was caused by the contributions of
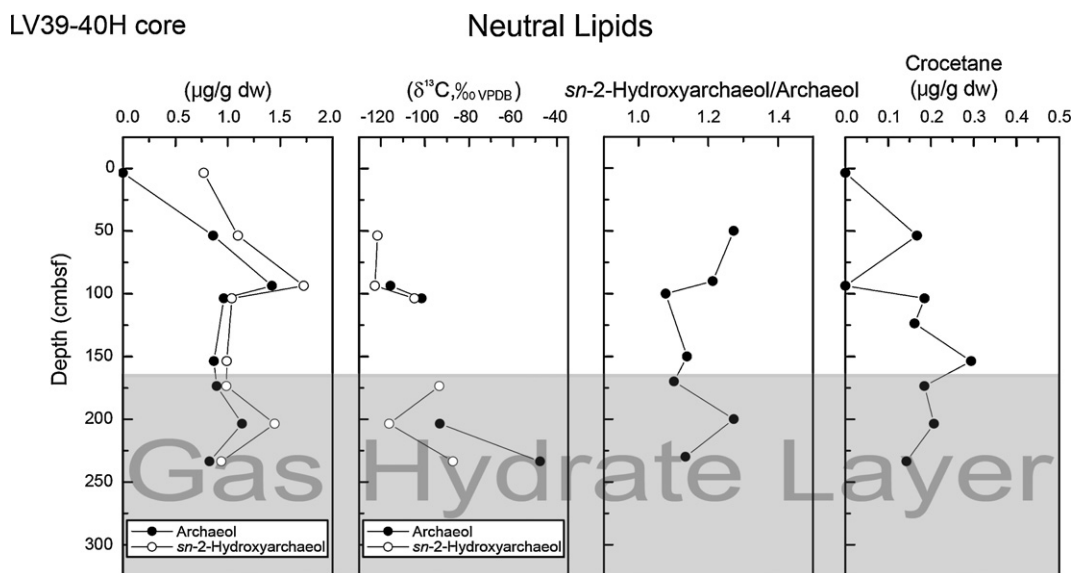
Figure 6. Depth profiles of the concentrations and $\delta^{13}C$ values of individual neutral lipids and the ratios of sn-2-hydroxyarchaeol relative to archaeol in the sediment core (LV39-40H) containing distinctive layers of gas hydrates (grey-shaded areas). Specific neutral lipids (sn-2-hydroxyarchaeol, archaeol, crocetane) in the LV39-30H core were not found, because their concentrations were below the detection limit.

the methanogenic archaea in the deep sediment layers and not the changes in the AOM ecotype (Fig. 6). This inference is in agreement with the heavier $\delta^{13}C$ values of the archaeol in the hydrate zone that were discussed above. On the other contrary, the peak concentrations of crocetane at a depth of 150–160 cmbsf in the LV39-40H cores were the robust biomarker for ANME-2 and were considered as results of the long-term preservation derived from the AOM activity of the ANME-2 (Thiel et al., 1999; Peckmann et al., 1999; Barber et al., 2001). It was recently proven that changes in the methane fluxes could influence the AOM community structure and the ANME-2 groups have a preferential niche in the habitats of elevated methane partial pressures (Nauhaus et al., 2002, 2005; Treude et al., 2003; Blumenberg et al., 2004). Therefore, a change in the ANME ecotypes from ANME-2 to ANME-1 species based on the crocetane concentration change in the sediment core (LV39-40H) can be explained by the adaptation of ANME-1 archaea to low methane partial pressure (Blumenberg et al., 2005).

5. Conclusions

This study focused on the characterization of the bulk organic matter, as well as the origin and specific lipid biomarkers related to the archaeal and bacterial aggregates involved in the anaerobic oxidation of methane (AOM) in a well-known cold seep environment in the Sea of Okhotsk. The origin of sedimentary organic matter is mostly the pelagic bacteria and algae. Specific archaeal lipid biomarkers were vertically detected in the LV39-40H cores, demonstrating considerable contribution of AOM-performing biomass to the bulk organic carbon corresponded with the negative excursion of the $\delta^{13}C_{org}$ at core depths of 90–100 cmbsf. The heavy carbon isotope value of the archaeol in the sediment from the hydrate zone supported the hypothesis that the microbially generated methane in the deep hydrate layers could support the hydrate formation and AOM populations.

References

Aiken, G.R., McKnight, D.M., Wershaw, R.L., MacCarthy, P., 1985. Humic Substances in Soil, Sediment, and Water: Geochemistry, Isolation, and Characterization. Wiley-Interscience, New York.

Aloisi, G., Bouloubassi, I., Heijs, S.K., Pancost, R.D., Pierre, C., Sinninghe Damsté, J.S., Gottschal, J.C., Forney, L.J., Rouchy, J.-M., 2002. CH₄-consuming microorganisms and the formation of carbonate crusts at cold-seeps. Earth and Planetary Science Letters 203, 195–203.

Aloisi, G., Wallmann, K., Bollwerk, S.M., Derkachev, A., Bohrmann, G., Suess, E., 2004. The effect of dissolved barium on biogeochemical processes at cold seeps. Geochimica et Cosmochimica Acta 68, 1735–1748.

Barber, C.J., Grice, K., Bastow, T.P., Alexander, R., Kagi, R.I., 2001. The identification of crocetane in Australian crude oils. Organic Geochemistry 32, 943–947.

Barnes, R.O., Goldberg, E.D., 1976. Methane production and consumption in anoxic marine sediments. Geology 4, 297–300.

Bian, L., Hinrichs, K.-U., Xie, T., Brassell, S.C., Iversen, N., Fossing, H., Jørgensen, B.B., Hayes, J.M., 2001. Algal and archaeal polyisoprenoids in a recent marine sediment: molecular isotopic evidence for anaerobic oxidation of methane. Geochemistry Geophysics Geosystems 2. doi:10.1029/2000GC000112.

Biebow, N., Huetten, E., 1999. Cruise Reports: KOMEX, I and II Editions. GEOMAR, Kiel.

Birgel, D., Himmler, T., Freiwald, A., Peckmann, J., 2008. A new constraint on the antiquity of anaerobic oxidation of methane: late Pennsylvanian seep limestones from southern Namibia. Geology 36, 543–546.

Blumenberg, M., Seifert, R., Reitner, J., Pape, T., Michaelis, W., 2004. Membrane lipid patterns typify distinct anaerobic methanotrophic consortia. Proceedings of the National Academy of Sciences of the United States of America 101, 11111–11116.

Blumenberg, M., Seifert, R., Nauhaus, K., Pape, T., Michaelis, W., 2005. In vitro study of lipid biosynthesis in an anaerobically methaneoxidising microbial mat. Applied and Environmental Microbiology 71, 4345–4351.

Boetius, A., Ravenschlag, K., Schubert, C.J., Rickert, D., Widdel, F., Gleseke, A., Amann, R., Jørgensen, B.B., Witte, U., Pfannkuche, O., 2000. A marine microbial consortium apparently mediating anaerobic oxidation of methane. Nature 407, 623–626.

Bogorov, V.G., 1974. Plankton Mirovogo Okeana (Plankton of the World Ocean). Nauka, Moscow.

Bolle, M.P., Pardo, A., Hinrichs, K.-U., Adatte, T., von Salis, K., Burns, S., Keller, G., Muzylev, 2000. The Paleocene-Eocene transition in the marginal northeastern Tethys (Kazakhstan and Uzbekistan). International Journal of Earth Sciences 89, 390–414.

Boon, J.J., de Leeuw, J.W., Hoeck, V.G., Vosjan, J.H., 1977. The significance of taxonomical value of iso- and anteiso-monoenic fatty acids and branched β-hydroxy acids in *Desulfovibrio desulfuricans*. Journal of Bacteriology 129, 1183–1191.

Bourbonniere, R.A., Meyers, P.A., 1996. Sedimentary geolipid records of historical changes in the watersheds and productivities of Lakes Ontario and Erie. Limnology and Oceanography 41, 352–359.

Bray, E.E., Evans, E.D., 1961. Distribution of n-paraffins as a clue to recognition of source beds. Geochimica et Cosmochimica Acta 22, 2–15.

Buffett, B., Archer, D., 2004. Global inventory of methane clathrate: sensitivity to changes in the deep ocean. Earth and Planetary Science Letters 227, 185–199.

Conrad, R., 2005. Quantification of methanogenic pathways using stable carbon isotopic signatures: a review and a proposal. Organic Geochemistry 36, 739–752.

Corrigan, D., Kloos, C., O'Connor, C.S., Timoney, R.F., 1973. Alkanes from four types of Sphagnum moss. Phytochemistry 12, 213–214.

Cragg, B.A., Parkes, R.J., Fry, J.C., Weightman, A.J., Rochelle, P.A., Maxwell, J.R., 1996. Bacterial populations and processes in sediments containing gas hydrates (ODP leg 146: Cascadia Margin). Earth and Planetary Science Letters 139, 497–507.

Deines, P., 1980. The isotopic composition of reduced organic carbon. In: Fritz, P., Fontes, J.C. (Eds.), Handbook of Environmental Isotope Geochemistry. The Terrestrial Environment, vol. 1.A. Elsevier, Amsterdam, pp. 329–406.

Derkachev, A.N., Bohrmann, G., Greinert, J., Mozherovskii, A.V., 2000. Authigenic carbonate and barite mineralization in sediments of the Deryugin basin (Sea of Okhotsk). Lithology and Mineral Resources 35, 504–519.

Dickens, G.R., 2003. Rethinking the global carbon cycle with a large, dynamic and microbially mediated gas hydrate capacitor. Earth and Planetary Science Letters 213, 169–183.

Dzierzewicz, Z., Cwalina, B., Kurkiewicz, S., Chodurek, E., Wilczok, T., 1996. Intraspecies variability of cellular fatty acids among soil and intestinal strains of *Desulfovibrio desulfuricans*. Applied and Environmental Microbiology 62, 3360–3365.

Edlund, A., Nichols, P.D., Roffey, R., White, D.C., 1985. Extractable and lipopolysaccharide fatty acid and hydroxy acid profiles from *Desulfovibrio* species. Journal of Lipid Research 26, 982–988.

Eglinton, G., Hamilton, R.J., 1963. The distribution of n-alkanes. In: Swain, T. (Ed.), Chemical Plant Taxonomy. Academic, San Diago, Calif, pp. 187–217.

Eglinton, G., Hamilton, R.J., 1967. Leaf epicuticular waxes. Science 156, 1322–1334.

Elvert, M., Suess, E., Whiticar, M.J., 1999. Anaerobic methane oxidation associated with marine gas hydrates: superlight C-isotopes from saturated and unsaturated C20 and C25 irregular isoprenoids. Naturwissenschaften 86, 295–300.

Elvert, M., Suess, E., Greinert, J., Whiticar, M.J., 2000. Archaea mediating anaerobic methane oxidation in deep-sea sediments at cold seeps of the eastern Aleutian subduction zone. Organic Geochemistry 31, 1175–1187.

Elvert, M., Greinert, J., Suess, E., Whiticar, M.J., 2001. Carbon isotopes of biomarkers derived from methane- oxidizing microbes at Hydrate Ridge, Cascadia convergent margin. In: Paull, C.K., Dillon, W.P. (Eds.), Natural Gas Hydrates: Occurrence, Distribution, and Dynamics. American Geophysical Union, Washington, DC, USA, pp. 115–129.

Elvert, M., Boetius, A., Knittel, K., Jørgensen, B.B., 2003. Characterization of specific membrane fatty acids as chemotaxonomic markers for sulfate-reducing bacteria involved in anaerobic oxidation of methane. Geomicrobiology Journal 20, 403–419.

Elvert, M., Hopmans, E.C., Treude, T., Boetius, A., Hinrichs, K.-U., 2005. Spatial variatons of archaeal-bacterial assambladges in gas hydrate bearing sediments at a cold seep: implications from a high resolution molecular and isotopic approach. Geobiology 3, 195–209.

Emerson, S., Hedges, J.I., 1988. Processes controlling the organic carbon content of open ocean sediments. Paleoceanography 3, 621–634.

Fehn, U., Snyder, G., Egeberg, P.K., 2000. Dating of pore waters with I-129: relevance for the origin of marine gas hydrates. Science 289, 2332–2335.

Feio, M.J., Beech, I.B., Carepo, M., Lopes, J.M., Cheung, C.W.S., Franco, R., Guezennec, J., Smith, J.R., Mitchell, J.I., Moura, J.J.G., Lino, A.R., 1998. Isolation and characterisation of a novel sulphate-reducing bacterium of the *Desulfovibrio* Genus. Anaerobe 4, 117–130.

Francois, R., Altabet, M.A., Goericke, R., McCorkle, D.C., Brunet, C., Poisson, A., 1993. Change in the $\delta^{13}C$ of surface water particulate organic matter across the

subtropical convergence in the SW Indian Ocean. Global Biogeochemical Cycles 7, 627–644.

Ginsburg, G.D., Soloviev, V.A., Cranston, R.E., Lorenson, T.D., Kvenvolden, K.A., 1993. Gas hydrates from the continental slope, offshore Sakhalin Island, Okhotsk Sea. Geo-Marine Letters 13, 41–48.

Girguis, P.R., Orphan, V.J., Hallam, S.J., DeLong, E.F., 2003. Growth and methane oxidation rate of anaerobic methanotrophic archaea in a contivuous-flow bioreactor. Applied and Environmental Microbiology 69, 5472–5482.

Greinert, J., Bollwerk, S.M., Derkachev, A., Bohrmann, G., Suess, E., 2002. Massive barite deposits and carbonate mineralization in the Derugin Basin, Sea of Okhotsk: precipitation process at cold vent sites. Earth and Planetary Science Letters 203, 165–180.

Hachikubo, A., Kosaka, T., Kida, M., Krylov, A., Sakagami, H., Minama, H., Takahashi, N., Shoji, H., 2007. Isotopic fractionation of methane and ethane hydrates between gas and hydrate phases. Geophysical Research Letters 34, L21502. doi:10.1029/2007GL030557.

Haeckel, M., Suess, E., Wallmann, K., Rickert, D., 2004. Rising methane gas bubbles form massive hydrate layers at the seafloor. Geochimica et Cosmochimica Acta 68, 4335–4345.

Haese, R.R., Meile, C., Van Cappellen, P., De Lange, G.J., 2003. Carbon geochemistry of cold seeps: methane fluxes and transformation in sediments from Kazan mud volcano, eastern Mediterranean Sea. Earth and Planetary Science Letters 212, 361–375.

Han, J., Calvin, M., 1969. Hydrocarbon distribution of algae and bacteria, and microbial activity in sediments. Proceedings of the National Academy of Sciences of the United States of America 64, 436–443.

Hinrichs, K.-U., Boetius, A., 2002. The anaerobic oxidation of methane: new insights in microbial ecology and biogeochemistry. In: Wefer, G., Billet, D., Hebbeln, D., Jørgensen, B.B., Schlüter, M., van Weering, T. (Eds.), Ocean Margin Systems. Springer Verlag, Heidelberg, Germany, pp. 457–477.

Hinrichs, K.-U., Hayes, J.M., Sylva, S.P., Brewer, P.G., DeLong, E.F., 1999. Methane-consuming archaebacteria in marine sediments. Nature 398, 802–805.

Hoefs, J., 1980. Stable Isotope Geochemistry. Springer-Ver-lag, Berlin.

Huang, Y., Lockheart, M.J., Collister, J.W., Eglington, G., 1995. Molecular and isotopic biochemistry of the Miocene Clarkia Formation: hydrocarbons and alcohols. Organic Geochemistry 23, 785–801.

Inagaki, F., Suzuki, M., Takai, K., Oida, H., Sakamoto, T., Aoki, K., Nealson, K.H., Horikoshi, K., 2003. Microbial communities associated with geological horizons in coastal subseafloor sediments from the Sea of Okhotsk. Applied and Environmental Microbiology 69, 7224–7235.

Ishiwatari, R., Uzaki, M., 1987. Diagenetic changes of lignin compounds in a more than 0.6 million-year old latchstring sediment (Lake Biwa, Japan). Geochimica et Cosmochimica Acta 51, 321–328.

Jasper, J.P., Gagosian, R.B., 1990. The sources and deposition of organic matter in the Late Quaternary Pygmy basin, Gulf of Mexico. Geochimica et Cosmochimica Acta 54, 1117–1132.

Jasper, J.P., Gagosian, R.B., 1993. The relationship between sedimentary organic carbon isotopic composition and organic biomarker compound concentration. Geochimica et Cosmochimica Acta 57, 167–186.

Jin, Y.K., Chung, K.H., Kim, Y., 2004. Geophysical investigation of gas hydrate-bearing sediments in the Sea of Okhotsk. Journal of the Korean Geophysical Society 7, 207–215.

Jin, Y.K., Obzhirov, A., Shoji, H., Mazurenko, L., 2007. Cruise reports: CHAOS, III Editions. RV Akademik M.A. Lavrentyev, Cruise 39, KOPRI.

Kaneda, T., 1991. Iso- and anteiso-fatty acids in bacteria: biosynthesis, function, and taxonomic significance. Microbiology Review 55, 288–302.

Keeling, C.D., Whorf, T.P., Wahlen, M., van der Plicht, J., 1995. Interannual extremes in the rate of rise of atmospheric carbon dioxide since 1980. Nature 375, 666–670.

Kimura, N., Wakatsuchi, M., 2000. Relationship between sea-ice motion and geostrophic wind in the Northern Hemisphere. Geophysical Research Letters 27, 2738–3735.

Knittel, K., Lösekann, T., Boetius, A., Kort, R., Amann, R., 2005. Diversity and distribution of methanotrophic archaea at cold seeps. Applied and Environmental Microbiology 71, 467–479.

Koblents-Mishke, O.I., 1967. Primary Production of the Pacific Ocean, Okeanologiya. Biologiya Tikhogo Okeana (Oceanology: Biology of the Pacific Ocean). Nauka, Moscow, part 1, pp. 62–65.

Kohring, L.L., Ringelberg, D.B., Devereux, R., Stahl, D.A., Mittelman, M.W., White, D.C., 1994. Comparison of phylogenetic relationships based on phospholipid fatty acid profiles and ribosomal RNA sequence similarities among dissimilatory sulfate-reducing bacteria. FEMS Microbiology Letters 119, 303–308.

Krishnamurthy, R.V., Bhattacharya, S.K., Kusumgar, S., 1986. Palaeoclimatic changes deduced from $^{13}C/^{12}C$ and C/N ratios of Karewa lake sediments, India. Nature 323, 150–152.

Lüdmann, T., Wong, H.K., 2003. Characteristics of gas hydrate occurrences associated with mud diapirism and gas escape structures in the northwestern Sea of Okhotsk. Marine Geology 201, 269–286.

Lembke, L., Tiedemann, R., Nuernberg, D., Biebow, N., Bubenshchikova, N., Segl, M., Kaiser, A., 2003. Impact of Amur Riverine discharge on sediment composition, primary productivity and nutrient utilization in the Okhotsk Sea. Geophysical Research Abstracts 5, 11878.

Lembke, L., Tiedemann, R., Nuernberg, D., Obzhirov, A., Dullo, C., 2007. Variable Holocene methane emissions from cold seeps in the Okhotsk Sea - links to seismo-tectonic activity? Geophysical Research Abstracts 9, 10177.

Luan, X., Jin, Y.K., Obzhirov, A., Yue, B., 2008. Characteristics of shallow gas hydrate in Okhotsk Sea. Science in China, Series D 51, 415–421.

Matveeva, T., Soloviev, V., Wallmann, K., Obzhirov, A., Biebow, N., Poort, J., Salomatin, A., Shoji, H., 2003. Geochemistry of gas hydrate accumulation offshore NE Sakhalin Island (the Sea of Okhotsk): results from the KOMEX-2002 cruise. Geo-Marine Letters 23, 278–288.

Mayer, L.M., 1994. Surface area control of organic carbon accumulation in continental shelf sediments. Geochimica et Cosmochimica Acta 58, 1271–1284.

Mazurenko, L.L., Soloviev, V.A., Matveeva, T., Shoji, H., Kaulio, V., Logvina, E., Minami, E., Hachikubo, A., Sakagami, H., 2005. Methane venting on the continental margin off NE Sakhalin: nature of gas, authigenic carbonates and gas hydrates. Geophysical Research Abstracts 7, 03841.

McCaffrey, M.A., Farrington, J.W., Repeta, D.J., 1991. The organic geochemistry of Peru margin surface sediments: II. Paleoenvironmental implications of hydrocarbon and alcohol profiles. Geochimica et Cosmochimica Acta 55, 483–498.

Meyers, P.A., Silliman, J.E., Shaw, T.J., 1996. Effects of turbidity flows on organic matter accumulation, sulfate reduction, and methane generation in deep-sea sediments in the Iberia Abyssal Plain. Organic Geochemistry 25, 69–78.

Moss, C.W., Lambert-Fair, M.A., 1989. Location of double bonds in monounsaturated fatty acids of Campylobacter cryaerophila with dimethyl Disulfide derivatives and combined gas chromatography-mass spectrometry. Journal of Clinical Microbiology 27, 1467–1470.

Nauhaus, K., Boetius, A., Krüger, M., Widdel, F., 2002. In vitro demonstration of anaerobic oxidation of methane coupled to sulfate reduction from a marine gas hydrate area. Environmental Microbiology 4, 296–305.

Nauhaus, K., Treude, T., Boetius, A., Krüger, M., 2005. Environmental regulation of the anaerobic oxidation of methane: comparison of ANME-I and ANME-II communities. Environmental Microbiology 7, 98–106.

Nauhaus, K., Albrecht, M., Elvert, M., Boetius, A., Widdel, F., 2007. In vitro cell growth of marine archaeal-bacterial consortia during anaerobic oxidation of methane with sulfate. Environmental Microbiology 9, 187–196.

Nichols, P.D., Guckert, J.B., White, D.C., 1986. Determination of monounsaturated fatty acid double-bond position and geometry for microbial monocultures and complex consortia by capillary GC–MS of their dimethyl disulphide derivatives. Journal of Microbiological Methods 5, 49–55.

Nichols, P.D., Volkman, J.K., Palmisano, A.C., Smith, G.A., White, D.C., 1988. Occurrence of an isoprenoid C25 diunsaturated alkane and high neutral lipid content in Antarctic sea-ice diatom communities. Journal of Phycology 24, 90–96.

Niemann, H., 2005. Rates and signatures of methane turnover in sediments of continental marhins. PhD thesis, University of Bremen, Bremen, Germany.

Niemann, H., Elvert, M., 2008. Diagnostic lipid biomarker and stable carbon isotope signatures of microbial communities mediating the anaerobic oxidation of methane with sulphate. Organic Geochemistry 39, 1668–1677.

Niemann, H., Elvert, M., Hovland, M., Orcutt, B., Judd, A.G., Suck, I., Gutt, J., Joye, S.B., Damm, E., Finster, K., Boetius, A., 2005. Methane emission and consumption at a North Sea gas seep (Tommeliten area). Biogeosciences 2, 335–351.

Niemann, H., Lösekann, T., de Beer, D., Elvert, M., Nadalig, T., Knittel, K., Amann, R., Sauter, E.J., Schlüter, M., Klages, M., Foucher, J.P., Boetius, A., 2006a. Novel microbial communities of the Haakon Mosby mud volcano and their role as a methane sink. Nature 443, 854–858.

Niemann, H., Duarte, J., Hensen, C., Omoregie, E., Magalhaes, V.H., Elvert, M., Pinheiro, L.M., Kopf, A., Boetius, A., 2006b. Microbial methane turnover at mud volcanoes of the Gulf of Cadiz. Geochimica et Cosmochimica Acta 70, 5336–5355.

Nott, C.J., Xie, S., Avsejs, L.A., Maddy, D., Chambers, F.M., Evershed, R.P., 2000. n-Alkane distributions in ombrotrophic mires as indicators of vegetation change related to climatic variation. Organic Geochemistry 31, 231–235.

Obzhirov, A., 1992. Gas-geochemical manifestations of gas-hydrates in the Sea of Okhotsk. Alaska Geology 21, 1–7.

Obzhirov, A., 1993. Gas Geochemical Fields of Near Bottom Water Layer of the Seas and Oceans (In Russian). Nauka, Moscow.

Obzhirov, A., Vereshchagina, O., Sosnin, V., Shakirov, R., Salyuk, A., Lammers, S., Suess, E., Biebow, N., Winckler, G., Druzhinin, V., 2002. Methane monitoring in waters of the eastern shelf and slope of Sakhalin (in Russian). Russian Geology and Geophysics 43, 605–612.

Obzhirov, A., Shakirov, R., Salyuk, A., Suess, E., Biebow, N., Salomatin, A., 2004. Relations between methane venting, geological structure and seismo-tectonics in the Okhotsk Sea. Geo-Marine Letters 24, 135–139.

Orcutt, B.N., Boetius, A., Elvert, M., Samarkin, V.A., Joye, S.B., 2005. Molecular biogeochemistry of sulfate reduction, methanogenesis and the anaerobic oxidation of methane at Gulf of Mexico cold seeps. Geochimica et Cosmochimica Acta 69, 4267–4281.

Orphan, V.J., House, C.H., Hinrichs, K.U., McKeegan, K.D., DeLong, E.F., 2001. Methane-consuming archaea revealed by directly coupled isotopic and phylohenetic analysis. Science 293, 484–487.

Orphan, V.J., House, C.H., Hinrichs, K.U., McKeegan, K.D., DeLong, E.F., 2002. Multiple archaeal groups mediate methane oxidation in anoxic cold seep sediments. Proceedings of the National Academy of Sciences of the United States of America 99, 7663–7668.

Pancost, R.D., Sinninghe Damsté, J.S., de Lint, S., van der Maarel, M.J.E.C., Gottschal, J.C., The MEDINAUT Shipboard Scientific Party, 2000. Biomarker evidence for widespread anaerobic methane oxidation in Mediterranean sediments by a consortium of methanogenic archaea and bacteria. Applied and Environmental Microbiology 66, 1126–1132.

Pancost, R.D., Hopmans, E.C., Sinninghe Damsté, J.S., The MEDINAUT Shipboard Scientific Party, 2001. Archaeal lipids in Mediterranean cold seeps: molecular proxies for anaerobic methane oxidation. Geochimica et Cosmochimica Acta 65, 1611–1627.

Parkes, R.J., Calder, A.G., 1985. The cellular fatty-acids of 3 strains of *Desulfobulbus*, a Propionate-Utilizing sulfate-reducing bacterium. FEMS Microbiology Ecology 31, 361–363.

Peckmann, J., Thiel, V., Michaelis, W., Clari, P., Gaillard, C., Martire, L., Reitner, J., 1999. Cold seep deposits of Beauvoisin (Oxfordian; southeastern France) and Marmorito (Miocene; northern Italy): microbially induced authigenic carbonates. International Journal of Earth Sciences 88, 60–75.

Pestrikova, N., Obzhirov, A., 2007. Ecological aspects of gas hydrate accumulations in the Sea of Okhotsk. Geophysical Research Abstracts 9, 00438.

Prahl, F.G., Bennett, J.T., Carpenter, R., 1980. The early diagenesis of aliphatic hydrocarbons and organic matter in sedimentary particulates from Dabob Bay, Washington. Geochimica et Cosmochimica Acta 44, 1967–1976.

Premuzic, E.T., Benkovitz, C.M., Graffney, J.S., Walsh, J.J., 1982. The nature and distribution of organic matter in the surface sediments of world oceans and seas. Organic Geochemistry 4, 63–77.

Rau, G.H., Takahashi, T., Des Marais, D.J., Repeta, D.J., Martin, J.H., 1992. The relationship between $\delta^{13}C$ of organic matter and $[CO_2(aq)]$ in ocean surface water: data from a JGOFS site in the northeast Atlantic Ocean and a model. Geochimica et Cosmochimica Acta 56, 1413–1419.

Reeburgh, W.S., 1996. "Soft spots" in the global methane budget. In: Lidstrom, M.E., Tabita, F.R. (Eds.), Microbial Growth on C1 Compounds. Kluwer Academic Publishers, Dordrecht, pp. 334–342.

Rieley, G., Collier, R.J., Jones, D.M., Eglinton, G., 1991. The biogeochemistry of Ellesmere Lake, UK, -I, source correlation of leaf wax inputs to the sedimentary lipid record. Organic Geochemistry 17, 901–912.

Sackett, W.M., 1978. Carbon and hydrogen isotope effects during the thermocatalytic production of hydrocarbons in laboratory simulation experiments. Geochimica et Cosmochimica Acta 42, 571–580.

Sahling, H., Galkin, S.V., Salyuk, A., Greinert, J., Foerstel, H., Piepenburg, D., Suess, E., 2003. Depth related structure and ecological significance of cold-seep communities — a case study from the Sea of Okhotsk. Deep-Sea Research Part I 50, 1391–1409.

Schouten, S., Rijpstra, W.I.C., Kok, M., Hopmans, E.C., Summons, R.E., Volkman, J.K., Sinninghe Damsté, J.S., 2001a. Molecular organic tracers of biogeochemical processes in a saline meromictic lake (Ace Lake). Geochimica et Cosmochimica Acta 65, 1629–1640.

Schouten, S., Wakeham, S.G., Sinninghe Damsté, J.S., 2001b. Anaerobic methane oxidation by archaea in the euxinic water column of the Black Sea. Organic Geochemistry 32, 1277–1281.

Seki, O., Yoshikawa, C., Nakatsuka, T., Kawamura, K., Wakatsuchi, M., 2006. Fluxes, source and transport of organic matter in the western Sea of Okhotsk: stable carbon isotopic ratios of *n*-alkanes and total organic carbon. Deep-Sea Research Part I 53, 253–270.

Shakirov, R., Obzhirov, A., Suess, E., 2004. Mud volcanoes and gas vents in the Okhotsk Sea area. Geo-Marine Letters 24, 140–149.

Shoji, H., Minami, H., Hachikubo, A., Sakagami, H., Hyakutake, K., Soloviev, V., Matveeva, T., Mazurenko, L., Kaulio, V., Gladysch, V., Logvina, E., Obzhirov, A., Baranov, B., Khlystov, O., Biebow, N., Poort, J., Jin, Y.K., Kim, Y., 2005. Hydrate-bearing structures in the Sea of Okhotsk. Eos, Transactions. American Geophysical Union 86, 13–18.

Soloviev, V.A., Ginsburg, G.D., Duglas, V.K., Cranston, R., Lorenson, T., Alekseev, I.A., Baranova, N.S., Ivanova, G.A., Kazazaev, V.P., Lobkov, V.A., Mashirov, G.Yu., Natorkhin, M.I., Obzhirov, A.I., Titaev, B.F., 1994. Gas hydrates of the Okhotsk Sea (in Russian). Otechestvennaya Geologiya 2, 10–16.

Suess, E., Torres, M.E., Bohrmann, G., Collier, R.W., Greinert, J., Linke, P., Rehder, G., Trchu, A., Wallmann, K., Winckler, G., Zuleger, E., 1999. Gas hydrate destabilization: enhanced dewatering, benthic material turnover and large methane plumes at the Cascadia convergent margin. Earth and Planetary Science Letters 170, 1–15.

Summons, R.E., Franzmann, P.D., Nichols, P.D., 1998. Carbon isotopic fractionation associated with methylotrophic methanogenesis. Organic Geochemistry 28, 465–475.

Teske, A., Hinrichs, K.U., Edgcomb, V., Gomez, A.D., Kysela, D., Sylva, S.P., Sogin, M.L., Jannasch, H.W., 2002. Microbial diversity of hydrothermal sediments in the Guaymas basin: evidence for anaerobic methanotrophic communities. Applied and Environmental Microbiology 68, 1994–2007.

Thiel, V., Peckmann, J., Seifert, R., Wehrung, P., Reitner, J., Michaelis, W., 1999. Highly isotopically depleted isoprenoids: molecular markers for ancient methane venting. Geochimica et Cosmochimica Acta 63, 3959–3966.

Thiel, V., Peckman, J., Richnow, H.H., Luth, U., Reitner, J., Michaelis, W., 2001. Molecular signals for anaerobic methane oxidation in Black Sea seep carbonates and microbial mat. Marine Chemistry 73, 97–112.

Treude, T., Boetius, A., Knittel, K., Wallmann, K., Jorgensen, B.B., 2003. Anaerobic oxidation of methane above gas hydrates at hydrate ridge, NE Pacific Ocean. Marine Ecology-Progress Series 264, 1–14.

Tulloch, A.P., 1976. Chemistry of higher plant waxes. In: Kolattukudy, P.E. (Ed.), Chemistry and Biochemistry of Natural Waxes. Elsevier, New York, pp. 290–349.

Vainshtein, M., Hippe, H., Kroppenstedt, R.M., 1992. Cellular fatty acid composition of *Desulfovibrio* species and its use in classification of sulfate-reducing bacteria. Systematic and Applied Microbiology 15, 554–566.

Valentine, D.L., 2002. Biogeochemistry and microbial ecology of methane oxidation in anoxic environments: a review. Antonie Van Leeuwenhoek International Journal of General and Molecular Microbiology 81, 271–282.

Valentine, D.L., Reeburgh, W.S., 2000. New perspectives on anaerobic methane oxidation. Environmental Microbiology 2, 477–484.

Volkman, J.K., Johns, R.B., Gillan, F.T., Perry, G.J., 1980. Microbial lipids of an intertidal sediment—I. Fatty acids and hydrocarbons. Geochimica et Cosmochimica Acta 44, 1133–1143.

Wallmann, K., Aloisi, G., Haeckel, M., Obzhirov, A., Pavlova, G., Tishchenko, P., 2006. Kinetics of organic matter degradation, microbial methane generation, and gas hydrate formation in anoxic marine sediments. Geochimica et Cosmochimica Acta 70, 3905–3927.

Wegener, G., Niemann, H., Elvert, M., Hinrichs, K.U., Boetius, A., 2008. Assimilation of methane and inorganic carbon by microbial communities mediating the anaerobic oxidation of methane. Environmental Microbiology 10, 2287–2298.

Wellsbury, P., Goodman, K., Barth, T., Cragg, B.A., Barnes, S.P., Parkes, R.J., 1997. Deep marine biosphere fueled by increasing organic matter availability during burial and heating. Nature 388, 573–576.

Werne, J.P., Baas, M., Sinninghe Damsté, J.S., 2002. Molecular isotopic tracing of carbon flow and trophic relationships in a methane-supported benthic microbial community. Limnology and Oceanography 47, 1694–1701.

Werne, J.P., Zitter, T., Haese, R.R., Aloisi, G., Bouloubassi, I., Heijs, S., Fiala-Médioni, A., Pancost, R.D., Sinninghe Damsté, J.S., de Lange, G., Forney, L.J., Gottschal, J.C., Foucher, J.-P., Mascle, J., Woodside, J., the MEDINAUT and MEDINETH Shipboard Scientific Parties, 2004. Life at cold seeps: a synthesis of ecological and biogeochemical data from Kazan mud volcano eastern Mediterranean Sea. Chemical Geology 205, 367–390.

Whiticar, M.J., 1999. Carbon and hydrogen isotope systematics of bacterial formation and oxidation of methane. Chemical Geology 161, 291–314.

Whiticar, M.J., Faber, E., Schoell, M., 1986. Biogenic methane formation in marine and freshwater environments: CO_2 reduction vs. acetate fermentation – isotope evidence. Geochimica et Cosmochimica Acta 50, 693–709.

Woltemate, I., Whiticar, M.J., Schoell, M., 1984. Carbon and hydrogen isotopic composition of bacterial methane in a shallow freshwater lake. Limnology and Oceanography 29, 985–992.

Wuebbles, D.J., Hayhoe, K., 2002. Atmospheric methane and global change. Earth-Science Reviews 57, 177–210.

Zonenshayn, L.P., Murdmaa, I.O., Baranov, B.V., Kuznetsov, A.P., Kuzin, V.S., Kuz'min, M.I., Avdeyko, G.P., Stunzhas, P.A., Lukashin, V.N., Barash, M.S., Valyashko, G.M., Demina, L.L., 1987. An underwater gas source in the Sea of Okhotsk west of Paramushir island. Oceanology 27, 598–602.